Effects of Raindrop Spectra on Cumulus Model

By
David A. Mathews

Department of Atmospheric Science
Colorado State University
Fort Collins, Colorado

Colorado
State
University

Department of
Atmospheric Science

Paper No. 174

EFFECTS OF RAINDROP SPECTRA ON A CUMULUS MODEL

by

David A. Matthews

Department of Atmospheric Science
Colorado State University
Fort Collins, Colorado

July 1971

Atmospheric Science Paper 174

ABSTRACT OF THESIS

EFFECTS OF RAINDROP SPECTRA ON A CUMULUS MODEL

A review of observed and theoretical raindrop
distributions is presented. From these drop spectra one
representative distribution is selected to determine if
a current cloud model (Orville, Liu, 1969) was sensitive
to the type of drop specra assumed in its hydrometeor
growth equations. The results of a series of experiments
using the selected drop spectra (Mueller, 1962b) and the
widely used drop spectra (Marshall, Palmer, 1948) showed
that the new drop spectra affected the parameterized
microphysics within the model significantly. Cloud water
content was increased from 10 to 100 percent of the
Marshall-Palmer values. The amount of increase was pro-
portional to the growth time of the cloud. Rain water
content of the new spectra was generally less than Marshall-
Palmer toward cloud top and greater than that of Marshall-
Palmer below mid-cloud levels. Rain water generally differed
from Marshall-Palmer values by 50 to 200 percent. Effects
above the model noise level due to different drop spectra
thus illustrate the need for further "fine tuning" of cloud
models to Nature's variables.

David A. Matthews
Atmospheric Sciences Department
Colorado State University
Fort Collins, Colorado 80521
June 1971

ACKNOWLEDGEMENTS

TABLE OF CONTENTS

TABLE OF CONTENTS (CONTINUED)

LIST OF TABLES

LIST OF FIGURES

I. INTRODUCTION

Background

Cloud modeling is becoming increasingly important to the development of physical meteorology and weather modification. Today cloud models are used to study phenomena of both the synoptic scale such as hurricanes (Gentry, Sheets, 1970) and the mesoscale such as hailstorms (Wisner, 1970).

However, Warner (1970) has pointed out an alarming disparity in the amounts of liquid water content and height of cloud tops predicted by one-dimensional steady state cloud models. Although Warner's criticism pertains to one-dimensional models, similar criticisms have been made of two-dimensional models. One topic of debate at the Second National Cloud Physics Conference in August 1970 was the lack of detailed verification of cloud microphysics of various current cloud models. A point has been reached in the development of cloud modeling where the detailed aspects of many basic assumptions upon which cloud models are based should now be examined.

One important assumption is the type and shape of the precipitation spectrum. Numerous studies of droplets and drop concentrations have revealed inverse exponential distributions of drop sizes per unit volume. Current cloud modeling research is based largely upon Kessler's (1969) parameterization of cloud microphysics which assume a Marshall-Palmer (1948) distribution of precipitation sizes.

However, many drop spectra which differ from the Marshall-Palmer (MP) have been observed in recent years.

Objectives

This thesis will (1) show that significantly different drop spectra are known to exist in nature and (2) determine if current empirical two-dimensional modeling methods for rain and cloud water are significantly sensitive to various assumed drop size distributions.

II. PROCEDURE

To provide a foundation for selecting a representative drop distribution, a thorough literature survey of theoretical and observed spectra is presented. This survey discusses the major theoretical and empirical findings of Marshall and Palmer (1948) and Gunn and Marshall (1958). These two distributions (MP, GM) are important because they are the foundation of many empirical equations relating to cloud microphysics and radar reflectivity. However, numerous other observations of drop spectra have been found that differ from the MP and GM distributions. Section 3 of this paper presents a detailed summary of these drop spectra.

From these spectra a set of data prepared from recent observations by Mueller (1963) has been selected to test the hypothesis that differences in distributions can significantly effect cloud modeling results. Mueller's work was selected because of the quality of his series of studies including large sample size, large geographical representation and objective measurement of drop spectra. Mueller's drop distributions were also chosen because they represented general features found by other observers. Details regarding the selection of Illinois State Water Survey distributions (Mueller, 1963) are presented in section 4.

Once the test distribution was selected, a cloud model was needed to test the hypothesis that empirical modeling

methods could be affected significantly by raindrop spectra types and shapes. A two-dimensional time dependant cloud model developed by Orville (1965) was selected as a test model. The appropriate hydrometeor growth equations were then derived using the Illinois State Water Survey raindrop spectra and added to the Orville Symmetric Cloud Model.

Experimentation with the cloud model using Illinois State Water Survey (hereafter, ISWS) drop spectra and Marshall-Palmer drop spectra was then performed. Several runs of the model using identical soundings, boundary conditions and initial conditions were made with changes only in the hydrometeor growth relations based first on the MP drop spectra, and second on the ISWS spectra.

Results of the experimentation with different drop spectra provided significant changes in both cloud and rain water profiles.

III. LITERATURE SURVEY OF RAINDROP DISTRIBUTIONS

Empirical Raindrop Distributions

Many different raindrop distributions have been studied
in different climates, in various types of precipitation,
and at various levels in clouds. Nearly all of the empirical
studies have been made at the ground using different observa-
tion methods ranging from dyed filter paper to photographs.
Most of the empirical drop spectra follow an inverse ex-
ponential law. This section presents a summary of drop
spectra observed in the tropics by Blanchard (1953), Mee
and Takeuchi (1968), Fujiwara (1968), and Mueller (1962).
Drop spectra observed in temperate latitudes by Mueller,
Fujiwara, Ohtake (1969, 1970), Marshall and Palmer (1948),
and Gunn and Marshall (1958) are also presented. The
Marshall-Palmer and Gunn-Marshall, and Mueller (ISWS) dis-
tributions were fitted to parameterized inverse exponential
equations. Both MP and GM distributions have been used
widely throughout cloud modeling and meteorological radar
relationships. Different physical effects upon drop dis-
tributions in various parts of a cloud have been discussed
by Adderly (1953), Battan (1953), Gunn (1953), Langmuir
(1948), Laws and Parsons (1943, Spilhause (1948) and Rigby,
Marshall and Hitchfeld (1954). Theoretical aspects of the
effects of coalescence, accretion, and evaporation on rain-
drop spectra also have been studied by Hardy (1963). This

study is presented to provide a theoretical comparison of spectra changes both in and below clouds to aid in explanation of observed drop spectra. Parameterized microphysics and radar relationships are also discussed to provide an understanding of the importance of drop spectra to these fundamental assumptions in cloud models.

Cloud models are briefly discussed to point out the general assumptions currently made by cloud models regarding precipitation processes. Most cloud models make the assumption that an "average" raindrop distribution can apply to all cases but the literature indicates that each cloud system has its own drop spectra; therefore, for a model to be accurate the model must use the correct drop spectra for the particular cloud being modeled. Determination of the correct spectra for any given cloud is beyond the scope of this paper. However, by comparing the MP spectra with another average spectra (ISWS), it is shown that changes in assumed drop spectra will produce significant differences in model results.

Marshall-Palmer Distribution

Marshall and Palmer (1948) measured surface raindrop distributions on dyed filter paper and correlated these with radar echoes, finding an exponential relationship.

$$N_D = N_o e^{-\lambda D} \qquad\qquad (1.1)$$

Where D is the diameter, $N_D \delta D$ is the number of drops of diameter between D and D + δD in a unit volume (number mm^{-1} m^{-3}), N_D for D = 0. Where:

$$N_o = 8.0 \times 10^3 \; mm^{-1} \, m^{-3}$$
$$\lambda = 41 \; R^{-.21}$$

Where R is the precipitation rate in mm hr^{-1}.

The relationship in equation (1.1) is valid only for drop diameters greater than 1.0 mm. The upper limit of this exponential distribution was explained through disintegration of large droplets due to the drag forces on large drops.

The Gunn-Marshall Distribution

Gunn and Marshall (1958) found that for snow the equation (1.1) was valid; the intercept being a function of precipitation rate R (mm hr^{-1}):

$$N_o = 3.8 \times 10^3 \; R^{-.87} \qquad mm^{-1} \, m^{-3}$$
$$= 25.5 \; R^{-.48}$$

The sampling techniques used by Gunn and Marshall utilized a horizontal sheet of angora wool in a shallow box exposed on the ground. Direct analysis of the size and number distribution of melted snow flakes produced a horizontal number distribution (N_h) which was then converted to a spatial distribution (N_D) by the relationship:

$$N_D = \frac{N_h}{V}$$
$$V = KD^{.31} \qquad \qquad V \; (cm \; sec^{-1})$$

V is the fall velocity (Langleben, 1954) of snowflakes having a melted diameter D and a coefficient K of 200 sec^{-3}.

Figure 1 illustrates the difference between snow and rain distributions shown by Gunn-Marshall (1958). For example we can see the variable intercept (N_o) for the Gunn-Marshall case (fig. la) in contrast to the constant N_o of the Marshall-Palmer case (fig. lc). The variation in terminal velocity of snow and rain used in conversion to spatial distributions (N_d) from N_H is illustrated in Figure lb. The small slope of the GM distribution for a rainfall rate of 2.5 mm hr^{-1} in contrast to the slope for MP at a rainfall rate of 100 mm hr^{-1} further illustrates the differences between these snowflake and raindrop distributions.

Imai et al. (1955) compared snow distributions for three periods of two-hour samples with the Marshall-Palmer distribution for average rain and found reasonably good agreement. Gunn-Marshall also found a similarly good fit with MP by treating their snow distributions in the same manner at low precipitation rates. Beyond 2 mm diameter, the rain and snow velocities maintain an almost constant ratio (fig. lb). Therefore the change in λ resulting from melting is negligible (Gunn-Marshall, 1958) which has been verified by Ohtake (1969) and others. Thus the slopes of the drop distributions above and below the melting level are identical.
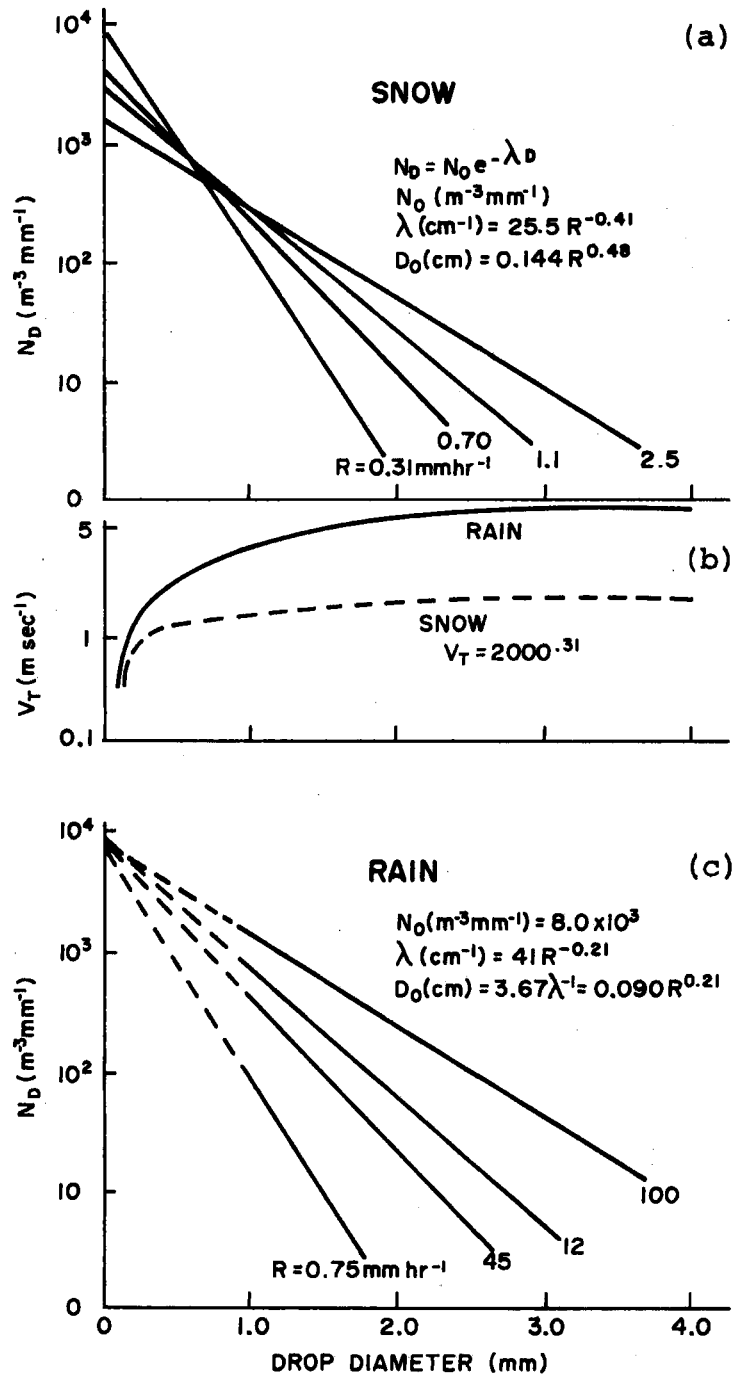
Fig. 1. A comparison between the Gunn-Marshall (a) and
Marshall-Palmer (c) distributions for various
precipitation rates (R) for snow and rain respec-
tively. Values of N_O, N_D, λ, and D_O are
defined in the figures. Raindrop and snowflake
terminal velocities for diameters corresponding
to the GM & MP distribution are shown in (b)
(after Gunn-Marshall, 1958).

Effects of Coalescence, Accretaion, Auto Conversion and Evaporation on Drop Spectra

A study by Hardy (1963) which assumed a steady mass flux of raindrops below the melting level found a significant effect on the drop spectra shape due to coalescence of raindrops, accretion of cloud droplets, and evaporation of precipitation particles. These results were in agreement with those first considered by Blanchard (1953). Hardy found that in the case of an initial distribution having a steep slope, considerable modification of the distribution occurs due to the above three processes (see fig. 2). Although the number of small droplets is considerably reduced by each process, the number of larger drops is increased by coalescence and accretion, but is decreased by evaporation.

In the case of a distribution with relatively small slope, the distribution was only slightly modified by the three processes. The depletion of cloud liquid water content increases as the slope of the distribution becomes larger. Evaporation also tends to increase as the slope of the distribution increases because large numbers of small particles (which rapidly evaporate) occur as the slope increases. Thus the shape of the initial drop distribution has a distinct effect upon the degree to which condensation, coalescence and accretion influence the final drop spectra.
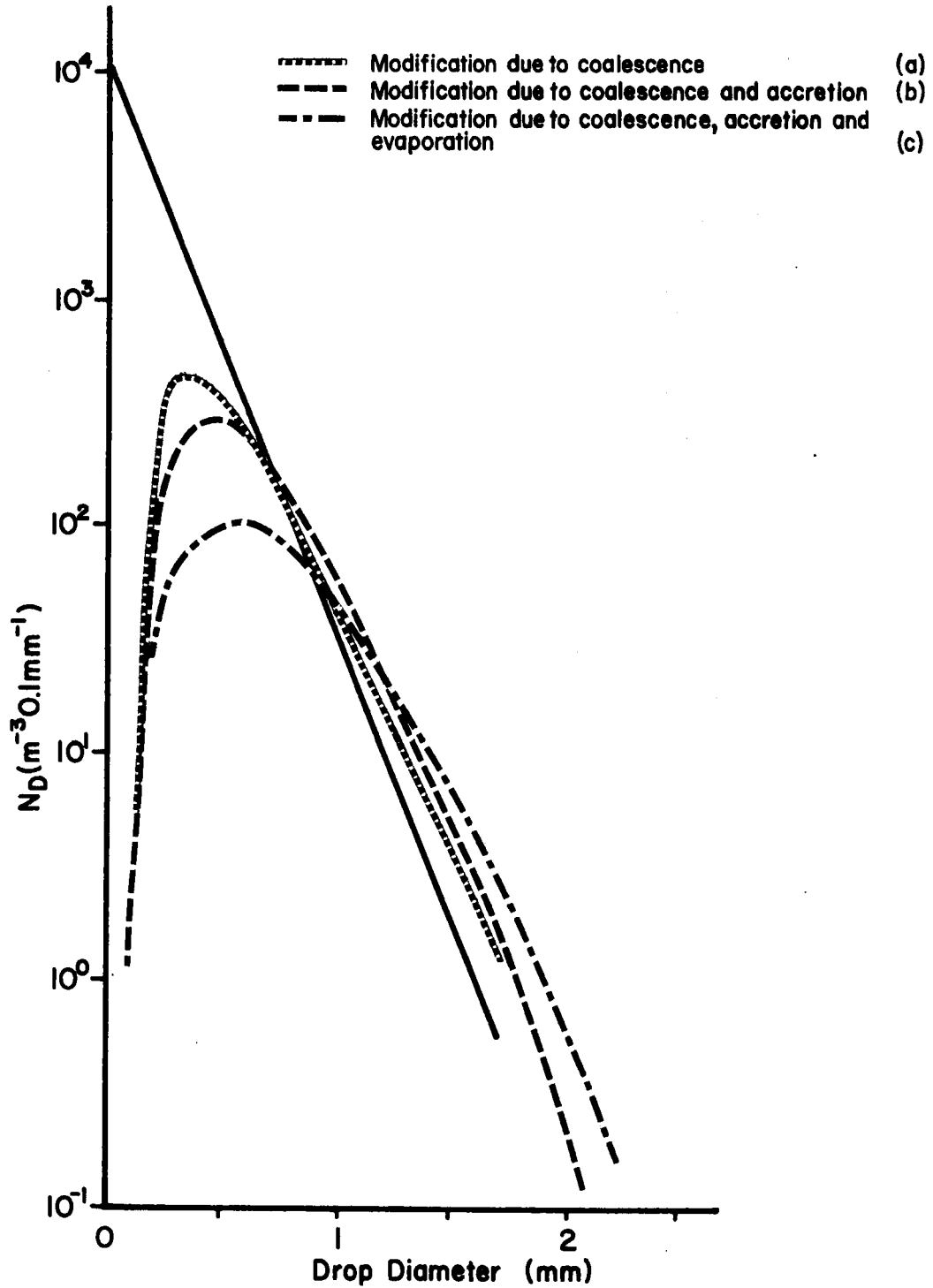
Fig. 2. A comparison of the effects of coalescence (a),
coalescence and accretion (b) coalescence, accre-
tion and evaporation (c) upon drops assuming an
initial MP distribution (solid line) after a fall
of 1 km through a cloud (a,b) and both a 1 km fall
through cloud plus 1 km fall beneath cloud base (c).

Hardy (1963) used the following relation for the effect

of accretion (collection) of cloud droplets by raindrops on

the raindrop diameter:

$$\frac{\Delta D}{\Delta t} = \frac{EM}{2\rho} V \qquad (1.2)$$

where rate of change of raindrop diameter ($\Delta D/\Delta t$) due to

accretion (collection) is a function of collection effici-

ency (E). Liquid Water Content (M), terminal velocity of

the raindrop (V), and density of water (ρ).

The relationship used to determine the effects of

evaporation on drop diameter was:

$$\frac{\Delta D}{\Delta t} \qquad \frac{2}{\rho MD^2} \frac{dM}{dt} \qquad (1.3)$$

where the rate of change of drop diameter ($\Delta D/\Delta t$) is a func-

tion of the rate of mass loss of the drop as a function of

time (dM/dt) as determined by Kinzer and Gunn (1951).

Gunn (1958) estimates that rainfall rates of 2.5 mm hr^{-1}

will deplete the original cloud liquid water content by 50%

within eleven minutes. Where as for a rainfall rate of 40

mm hr^{-1} that time is reduced to 2 minutes. These estimates

show that the rainfall rate is an important factor in the

life of a cloud. The rainfall rate is partly a function of

the processes of condensation, coalescence, accretion and

evaporation which depend upon the initial drop spectra as

illustrated by equations 1.1, 1.2 and 1.3.

Autoconversion is a widely used parameterized method of cloud microphysics (Kessler, 1969). Autoconversion is a method of converting cloud water to rainwater without direct calculation of the processes of coalescence and accretion. A threshold value of liquid water is assumed for rainwater. All water within the cloud below this threshold is considered cloud water and above it is rainwater. Rainwater can then be developed by processes of accretion and be depleted by evaporation.

Kessler (1969) found that growth by accretion in the presence of small water contents in the upper portions of strong updrafts causes overwhelming dilution of initial particle concentrations. This dilution is associated with horizontal spreading of particles and increasing average vertical separation between particles during their descent. He assumed a MP distribution of drop sizes in his model of hydrometeor growth. He related the total number of particles per unit volume to their mass distribution and the liquid water content which was conserved in his system. The precipitation fall speed was then related to the median diameter particle such that all precipitation falls at the same rate. The rainfall rate in his model is based on the liquid water content and precipitation terminal velocity V_o of the median diameter particle as related by:

$$V_o = 38.3 \; N_o^{1/8} \; M^{1/8} \; EXP \; (KZ/2) \qquad (m \; sec^{-1})$$

where V_o varies slowly with N_o and the total precipitable
water content M, as defined by the distribution for the
median drop diameter. The rainfall rate (R) is related to M
and V as follows:

$$R = M \cdot V_o \qquad [gm\ m^{-2}\ sec^{-1}]$$
$$= 3.6\ M \cdot V_o \qquad [mm\ hr^{-1}]$$
$$= 18.35\ M^{9/8} \qquad [mm\ hr^{-1}]$$

Here again the MP distribution is directly related to V as
defined above.

Another widely used relationship, the reflectivity
factor Z (which is used to determine the rainfall rate and
radar observations and predict radar reflectivity in cloud
models) is related to the drop distribution by:

$$Z = \int N_o D^6\ dD$$

where N = equation (1.1)

thus $Z = N_o e^{-\lambda D^6}\ dD$

whose solution is:

$$Z = 720\ \frac{N_o}{\lambda^7} \qquad (mm^6\ m^{-3})$$

where $\lambda = 42.1\ N_0^{1/8}\ M^{1/8} \qquad (m^{-1})$

The importance of an accurate distribution function of
drop sizes to both cloud physics and radar meteorology is
readily seen in the above fundamental relationships.

Fujiwara (1968) has made a study of various raindrop distributions at the surface and compared these with radar reflectivity and rainfall rates. He found that the reflectivity deviates from that predicted by the Z-R relation using the MP distribution. The Z-R relation was found to vary with the type of precipitation as shown in Table 1 where:

$$Z = a R^b \qquad (1.4)$$

Table 1. A Comparison of the Marshall-Palmer (1948) Z-R Relation With Those Observed by Fujiwara (1968) for Various Precipitation Types.

Precipitation Type	a	b
Thunderstorm	450	1.46
Rainshower	300	1.37
Continuous Rain	205	1.48
Marshall-Palmer	200	1.60

An example of the type of drop spectra upon which the values of Table 1 were determined is shown in Figure 9.

Consideration of the initial droplet spectra is also important because it will affect the rate of precipitation development and spectra slope. Warner (1969) has studied the general features of the droplet spectrum and its relation to both cloud nuclei and updraft speeds. He found that turbulence in the updraft does not broaden the droplet size distribution markedly beyond that produced by condensation

in a steady updraft. Under certain updraft conditions involving accretion, a spectrum broadening occurs. This may be explained by the repeated activation of fresh nuclei which produce a bimodal drop size distribution consisting of both older large drops formed by accretion and newer small drops formed by condensation on fresh nuclei. The bimodal precipitation distribution observed by Mueller (1962) may be explained by this process in cumulus clouds. Warner has also been able to reproduce the droplet spectra normally found at heights greater than 100 m above cloud base when proper collection coefficients and realistic updrafts are assumed.

In a study of seeded and unseeded showers in Arizona utilizing photographic images of drops Jones et al. (1968) found drop spectra whose concentrations could be related to four processes. These processes were: (1) artificial nucleation of clouds, (2) natural seeding by ice crystals falling from anvils of earlier or near by thunderstorms into the observed clouds, (3) self glaciation of stable rain falling from decaying thunderstorms, and (4) seeding from burning large masses of tree products (air pollution). Jones has shown that seeded clouds tend to have a drop distribution characterized by many small drops and fewer large drops than the distribution for natural clouds. This is expected by

microphysical effects of seeding which create a distribution
having large numbers of small drops.

Cloud Modeling and Drop Spectra

Most recent models including Orville (1969), Davis,
Weinstein (1967), Weinstein (1968), Simpson-Wiggert (1969),
and Murray (1971) assume an inverse exponential drop size
distribution of precipitation based upon the Marshall-Palmer
distribution. Much of the theoretical development of current
cloud model microphysics is based upon Kessler's (1969)
parameterized treatment of autoconversion, and hydrometeor
growth (accretion). Hydrometeor growth (discussed in detail
in section 5) is a direct function of the drop size spectra
assumed for the raindrop distribution.

Orville and Liu (1969) have used a model to study
cumulus dynamics and the effect of different precipitation
parameters for autoconversion and evaporation on cloud
growth. Their numerical model shows that the precipitation
process affects the early stages of the cloud very little;
however, it does affect the later stages significantly when
the precipitation tends to dissipate clouds.

In the Orville model there are two ways in which
clouds can dissipate; one is by the transformation of cloud
water content to rain water via autoconversion and accretion
processes which result in rain from the cloud base. The

second process is by stimulation of downdrafts due to the
evaporational cooling of rainwater below cloud base and
along its sides. The distribution of drop sizes is im-
portant to model dynamics because the effect of "water
loading" and unloading via precipitation is directly re-
lated to the precipitation size distribution of terminal
velocities. Orville uses both Berry's (1968) and Kessler's
(1969) techniques of autoconversion which are based upon
the M.P. distribution.

Tropical Raindrop Spectra

Drop size distributions were obtained by Blanchard
(1953) in Hawaii for non-orographic clouds of thunderstorms
and cyclones as well as the orographic clouds. He found
that the distribution of drops arriving at a horizontal
surface is skewed with a long tapering tail reaching into
the region of large drops. He noted that in this region
the distribution has so few drops that the number is statis-
tically inadequate. Thus because the very large drops con-
tain most of the precipitation water, incorrect intensities
can be calculated from data in error within large drop size
regions. In the case of Hawaiian orographic clouds where
there is a small standard deviation and largest drops
seldom are greater than 2 mm, this error was not considered
important.

Examination of sub-cloud drop-size distributions by Blanchard (1953) shows that they may not be representative of in-cloud distributions. Theoretical studies by Hardy (1963) support this observation which is important because most spectra reported in the literature are observed well below cloud base. The changes in sub-cloud distribution depend upon the fall distance, temperature, relative humidity, relative drop size, and wind shear. Blanchard's observations were made either at cloud base or at some point within the cloud system as it intercepted a mountain.

In semi-tropical orographic rains, many thousands of droplets per cubic meter were normally observed smaller than 0.5 mm diameter by Blanchard (1953) at cloud base. These may evaporate completely during a sub-cloud fall of 1000 m. These distributions differ from the MP drop distribution (fig. 3) presented in the literature.

Blanchard found that in general the number of drops per m^3 at the lower end of the raindrop spectrum is an inverse function of rain intensity and that the number of large drops is a direct function of intensity. These distributions may be the result of condensation first on large salt particles; then growth may occur by accretion processes with numerous cloud droplets. The median volume diameter of a given rainfall intensity in orographic rain is about half that found in thunderstorms and frontal rains (Blanchard, 1953).

10^4
10^3
10^2
10
10^0

2 3

1 2 3

N_D $(m^{-3} 0.2 mm^{-1})$

10^4
10^3
10^2
10
10^0

4 5 6 7

1 2 3

CURVE	R (mm hr^{-1})
1	.39
2	1.2
3	2.3
4	1.1
5	3.3
6	8.5
7	20.8
8	.84
9	20.1

10^4
10^3
10^2
10
10^0

8 9

1 2 3

DROP DIAMETER (mm)
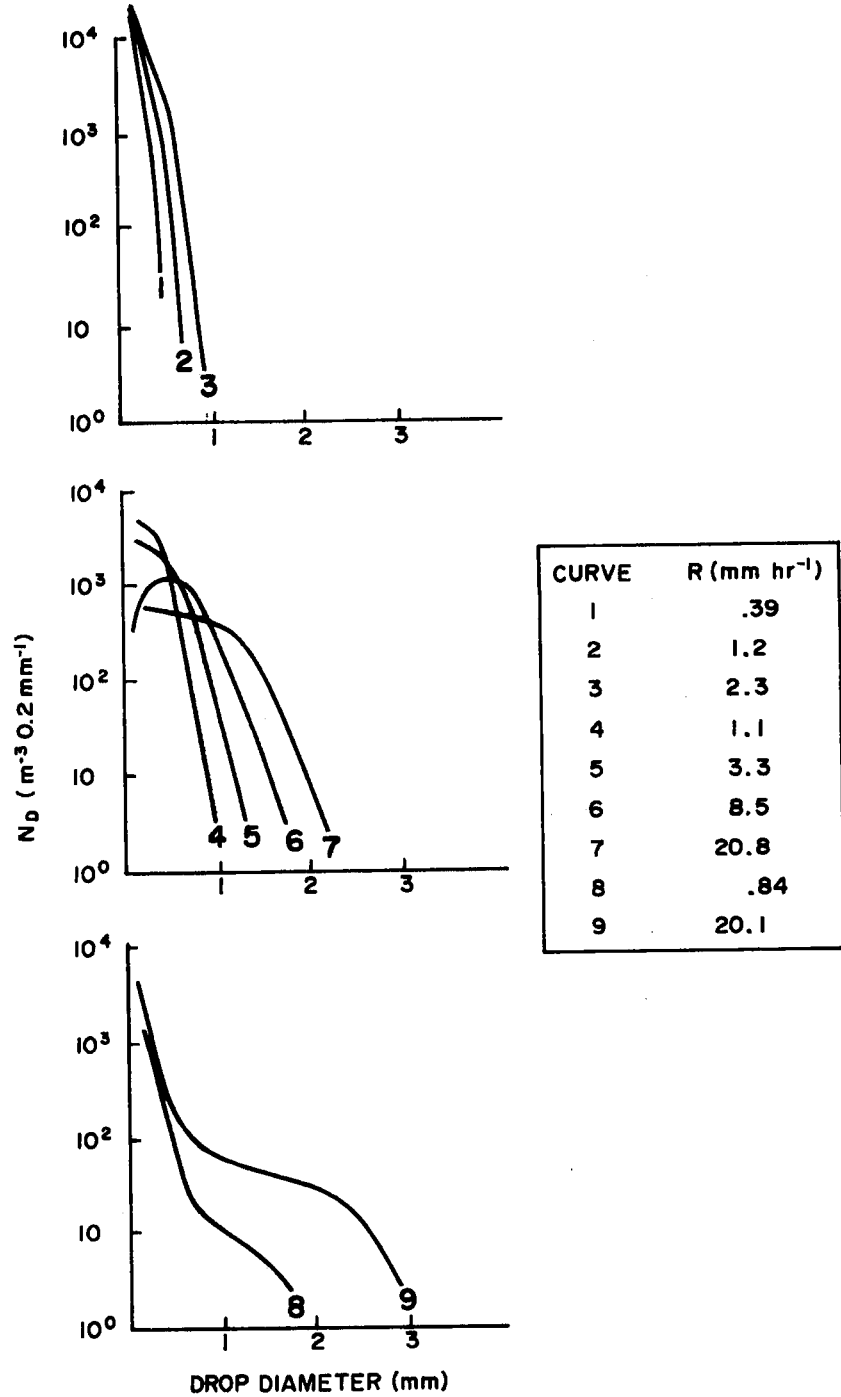
Fig. 3. Average raindrop distributions of tropical precipitation. Curves 1 - 3 taken at edge of nonfreezing orographic clouds. Curves 4 - 7 taken at cloud base. Curves 8 - 9 are non-orographic rain distributions (Blanchard, 1953).

Blanchard showed that the regression equation for D,
M, Z, the intercept diameter, liquid water content, and
reflectivity are functions of the rainfall rate R. These
relations were used to illustrate the basic difference be-
tween orographic rain from non-freezing clouds and rain as
a result of the Bergeron-Findeisen process.

He has summarized his observations as shown in Figure
3, where the observations of Hawaiian rain have been aver-
aged into three general classes: those taken at the cloud
base, and non-orographic rain distribution. It can be seen
that the distributions well up in the cloud (lines 3, 5)
are sharply different for those of the same rain intensity
at cloud base. The number of small size drops (2 mm or
smaller) is an order of magnitude greater inside the cloud
than at cloud base. While the numbers of .6 to .8 mm
diameter are an order of magnitude smaller within the cloud
than at cloud base. Another feature noted by Blanchard was
that a high rainfall intensities there are small numbers of
small drops which could be attributed to accretion with large
drops, whereas in cases of low rainfall rates a fall of over
1000 m beneath cloud base may evaporate all small drops.

Aircraft observation of marine tropical cumulus near
Puerto Rico measured raindrop sizes at all levels in clouds
probed (Mee and Takeuchi, 1968). The results showed that

the size distribution very closely follows that predicted by the M-P distribution except that there were always fewer particles in size categories smaller than 2 mm than was predicted. This departure was also observed by Marshall and Palmer (1948). Better agreement was found from high level samples in well developed clouds than from low level samples in small clouds. These observations generally agree with those of Blanchard in Figure 3.

These tropical cumulus observations showed that as liquid water content increased and height in cloud increased the M-P distribution more nearly approximated the observed precipitation drop spectra. Figure 4 illustrates the change in drop spectra at four observation levels. (o.6, 2, 4 and 6 km) in those observed tropical marine cumulus clouds. At the 6 km level the MP drop spectra very nearly approximates the observed spectra; however, all lower level cases depart from the MP case at drop diameters below 1 mm as did the original MP data. Flights 3 to 4 miles inland showed distinct changes from the broad marine distribution having only 50 drops per cm to a narrow continental drop distribution of 200 drops per cm . This sharp contrast in drop spectra confirms the difference between maritime and continental clouds (see Fletcher, 1952).
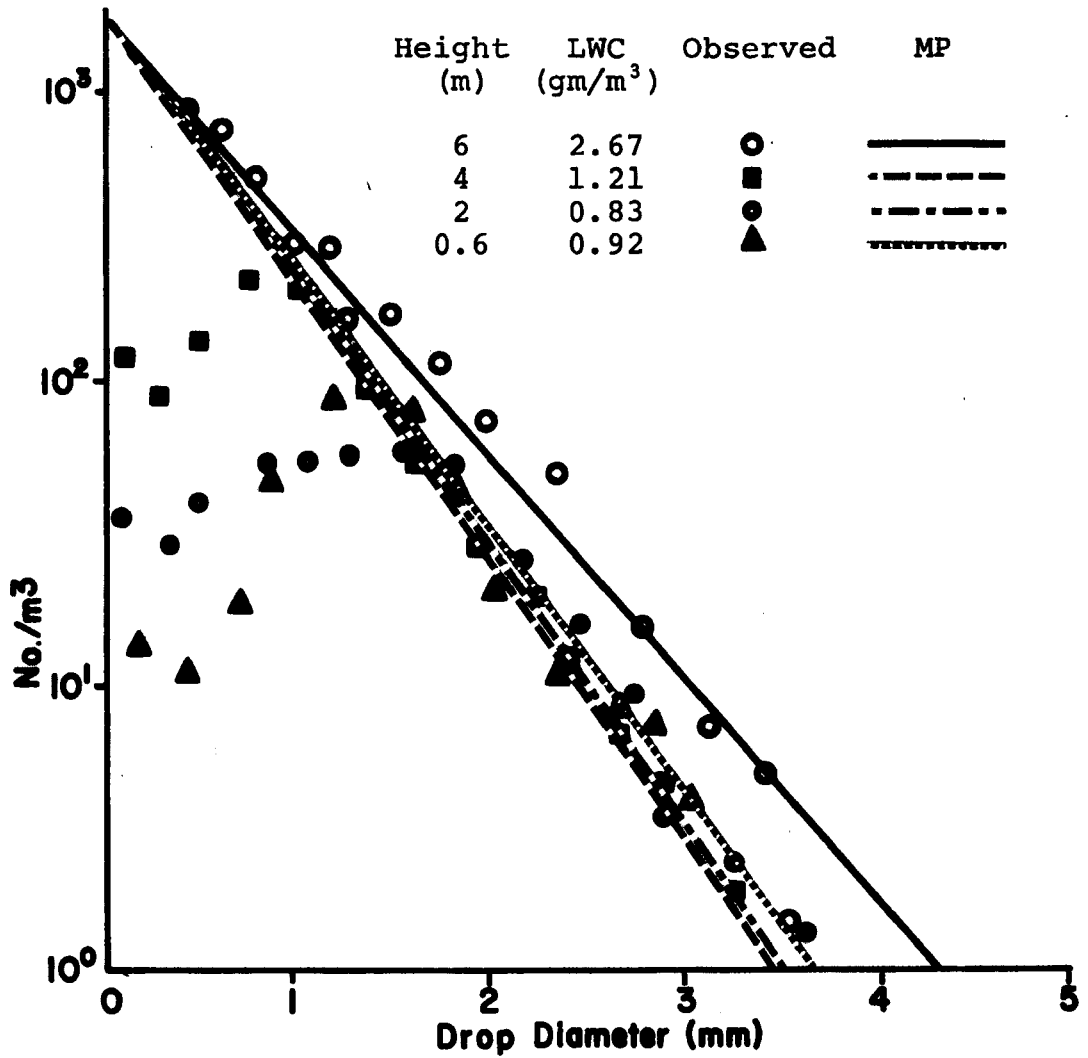
Fig. 4. Aircraft measurements of raindrop spectra in tropical clouds at 4 levels from cloud base (.6 km) to cloud top (6 km). Straight lines correspond to MP distribution predicted for given liquid water contents.

The instrumentation on the M.R.I. twin engine Aztec instrumented cloud physics aircraft included a continuous particle sampler using formvar replication, and a continuous hydrometeor sampler that collects particles greater than 100 mm in diameter with a collection efficiency of nearly 100%. This sampler utilized soft aluminum foil three inches wide and had a shutter speed of .5 seconds which was activated every 2.2 seconds.

The Illinois State Water Survey (Mueller, 1962) has made a series of observations of surface raindrop spectra using a raindrop camera. They found that their drop spectra could be accurately fitted by the following relationship:

$$N_D = \alpha D^2 e^{-\beta (D-D_o)^3}$$

where α, β are regression fitting parameters, N_D is the number of droplets between diameter D and $D + \delta D$, and D_o is the number associated with the mode of the distribution. Figure 5 shows the distribution fitted by the above relationship and their β parameter for Miami (N_s represents the number of cubic meters represented in the sample while N_t gives the total average number of drops per m^3).

From Table 2 we can see that there is very little continuity to the fitting parameters of the observed distribution as a function of rainfall rate. At larger rainfall
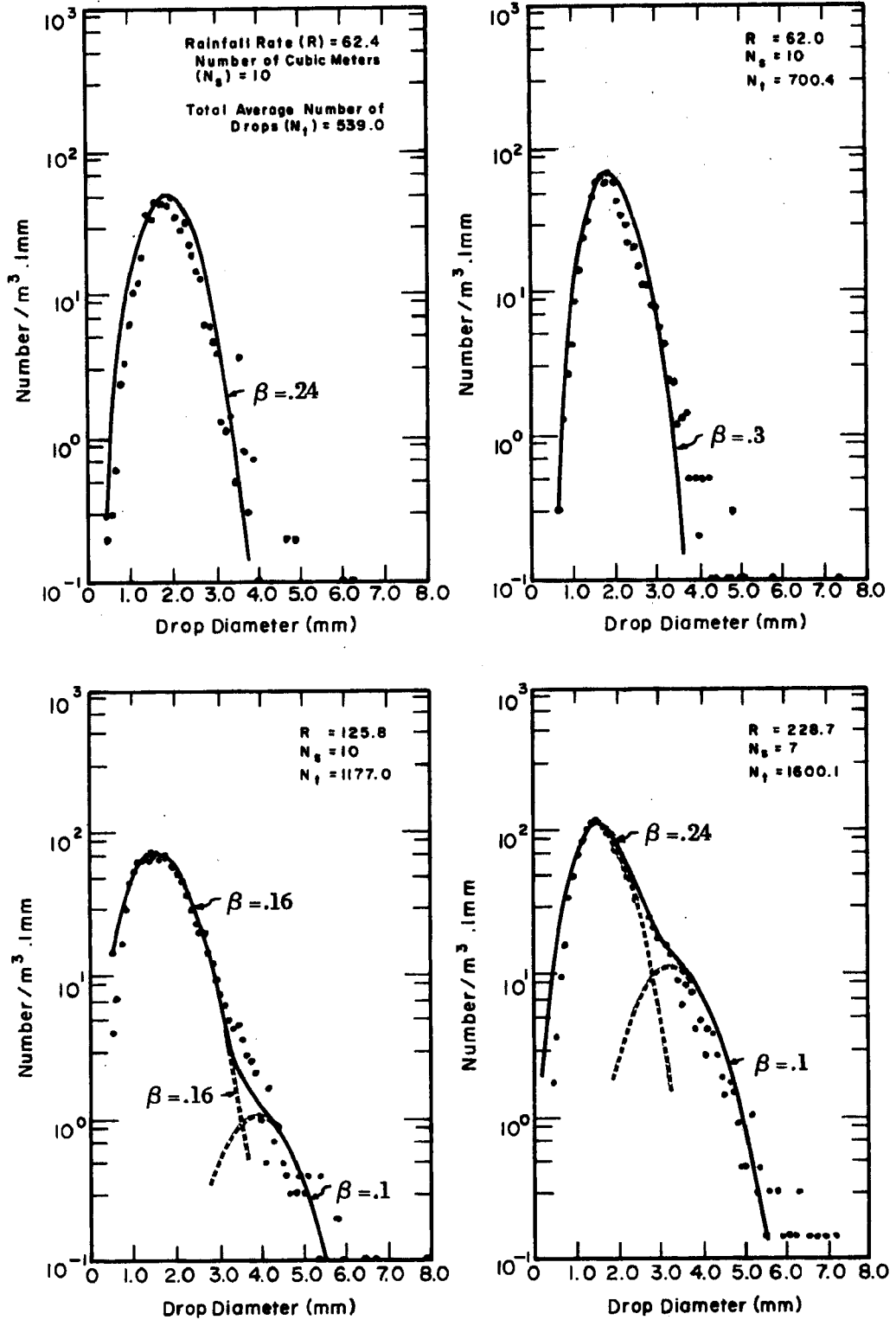
Fig. 5. Observed drop size distributions with empirical fitting distributions for rainshowers at Miami, Florida (after Mueller, 1962a).

rates one curve does not fit the data adequately; therefore,
a bimodal fit is made by a second curve for the larger drop
sizes (fig. 5). This lesser mode can be attributed to:
(1) interactions between two convective cells, (2) a second
generation level, (3) a different drop break up process or
(4) introduction of different cloud nuclei as mentioned
above (Jones et al., 1968). There is no direct evidence
of a pattern to the lesser mode occurrence in the Illinois

Table 2. Fitting Coefficients for Average
Distributions from Miami, Florida.

Rainfall Rate (mm/hr)	D_O (mm)	Fitting Coefficients		Coalescence Equation $(n/m^3 .1 mm)$	From Data $(n/m^3 .1 mm)$	%Error in N_t
		α	β			
2.1	.4	23.5	1.0	78.5	77.6	+ 1.16
3.65	.3	13.2	.5	88	87.7	+ .34
6.7	.1	14.5	.3	161	133	+21.00
9.29	.6	47.5	1.0	158	158	0
13.3	.7	80	1.0	267	228	+17.1
19.8	.8	87.5	1.0	292	286	+ 2.1
23.1	.8	105	1.0	350	334	+ 4.8
27.3	.8	112	1.0	374	360	+ 3.9
34.1	.6	59	.5	394	413	- 4.6
35.2	.8	120	1.0	400	394	+ 1.5
36.9	.3	49	.3	543	466	+16.5
40.0	.9	150	1.0	500	467	+ 7.05
43.5	1.0	125	1.0	417	411	+ 1.46
45.2	.4	49	.3	545	490	+11.2
52.1	.5	52	.3	578	540	+ 7.04
55.8	.4	40	.24	555	527	+ 5.31
62.4	.4	45	.24	625	539	+16.0
82.0	.5	68	.3	868	700	+24.0
125.8	0	58	.16	1210	1177	+ 2.8
228.7	.1	120	.24	1800	1600	+12.5

State Water Survey data thus indicating that more information is needed to determine a direct physical process for its generation. Fujiwara (1968) found bimodal distributions during the transient periods between cells. He suggested that the bimodal distribution was caused by cells having different stages of development. Figure 5a illustrates the transient bimodal distributions for two cases. From 1431-1435 and 1615-1623 LST bimodal distributions developed.

Temperate Latitude Drop Spectra

Simultaneous observations of snowflakes and raindrops at altitudes above and below the melting level along mountain slopes in Japan and Alaska (Ohtake, 1969) yielded average snow and rain distributions which generally agreed with the Gunn-Marshall (GM) distribution and occasionally agreed with Marshall-Palmer (MP) distributions. However, individual distributions differed from both GM and MP distributions. Ohtake found that these individual melted snowflake distributions were nearly identical to simultaneous raindrop distributions. He concluded that the snowflakes did not break up into several smaller drops upon melting. If the two drop distributions are the same, then the drop distributions resulting from the cold rain processes are determined by the type of snowflake distribution. Snowflake types depend upon the supersaturation and temperature (Nakaya, 1951); therefore,
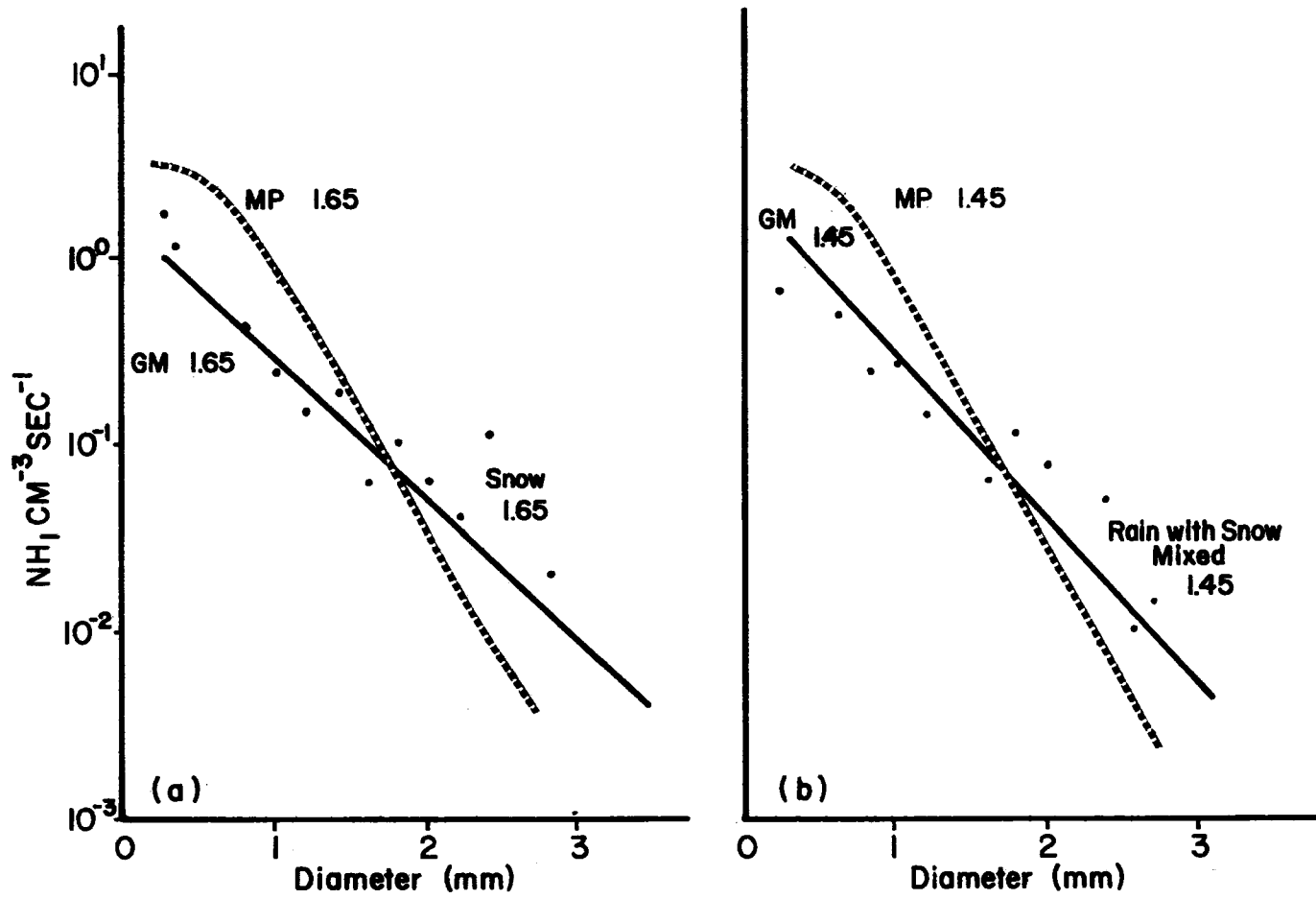
Fig. 6. A comparison of observed horizontal drop spectra with horizontal MP and GM spectra. (a) Observed equivalent melted drop spectra for plane dentrites in Alaska, $R = 1.65$ mm hr^{-1}, $T = 0.5^{o}$ C. (b) Same as for rain and snow mixed, $R = 1.45$ mm hr^{-1}, $T = 2.2^{o}$ C (after Ohtake, 1969).

the vertical profile of temperature and relative humidity above the melting level may determine the type of snowflake distribution and hence the type of raindrop distribution below the melting level.

Field observations have shown that drop distributions from the cold rain process differ from the GM and MP distributions. Distributions of melted snowflakes composed of plane dentrites in Alaska and Japan were less steep than GM distributions of comparable precipitation ratio (see fig. 6a, Ohtake, 1969). In contrast, Ohtake found that needle snowflakes agreed with MP distributions of comparable rainfall rates (fig. 6b).

Direct comparison of soundings of temperature and relative humidity with drop distributions adds further evidence that their vertical profile affects the melted raindrop spectrum (Ohtake, 1970). Ohtake found that most rain samples had size distributions similar to or less steep than GM when the atmosphere was almost saturated throughout the upper levels, having temperatures of -8 to -17° C. These conditions correspond to those of Nakaya for crystal shapes of plane dentrites, section plates, and plates (fig. 7a). Distributions of raindrops which were similar to MP were found with saturated upper-air conditions in the temperature range of 0 to -10° C., which corresponds to needles, irregular

(7a)

(7b)
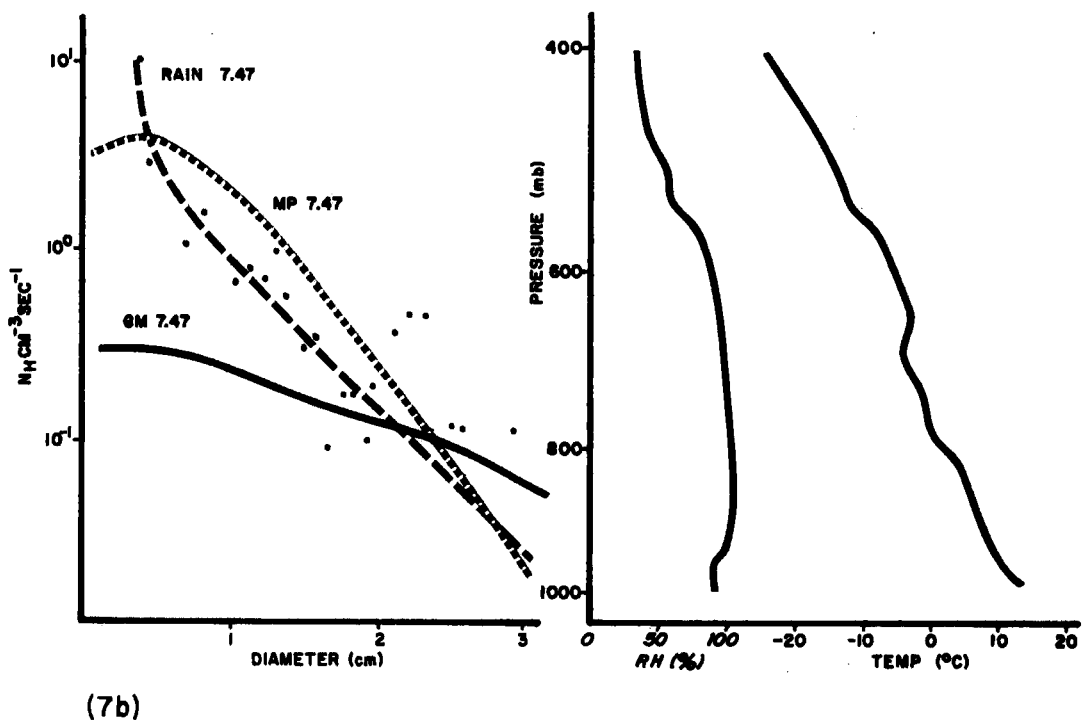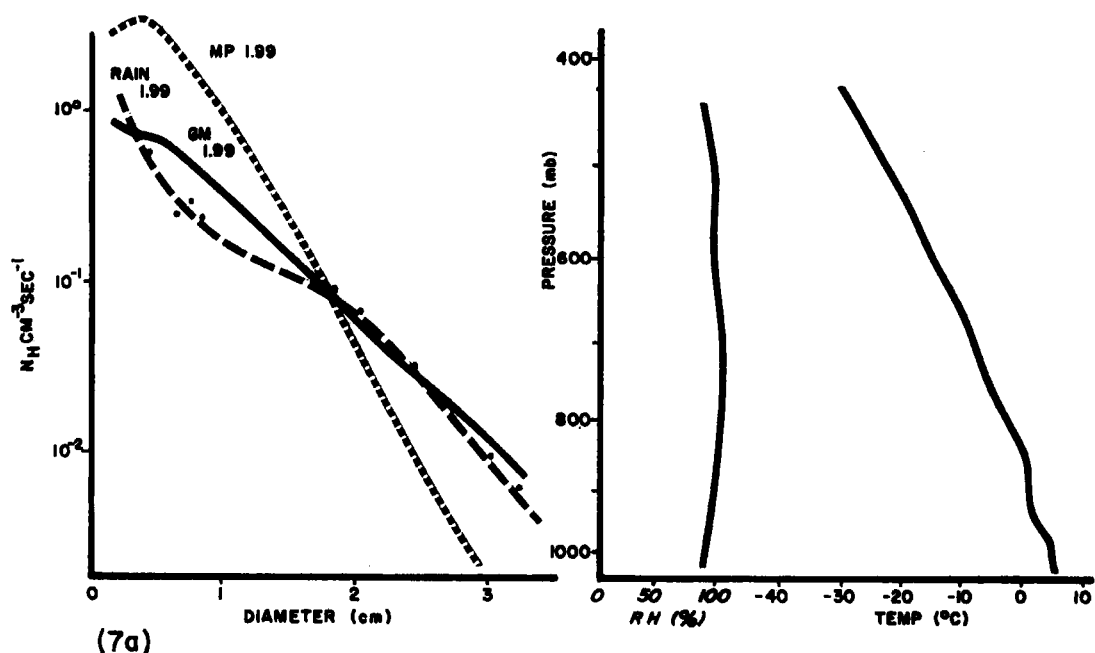
Fig. 7. (a)   Comparison of observed horizontal drop spectra
with horizontal MP and GM spectra. 4 April 1960,
Sendai, Japan; R = 1.99 mm hr⁻¹ , T = 4.7⁰ C.
(b)   Same as (a) for 12 August 1967, College,
Alaska, R = 7.47 mm hr⁻¹ , T = 12.5⁰ C. Soundings
corresponding to drop spectra times are shown on
right (after Ohtake, 1970).

needles, and scroll or cup crystals according to the Nakaya
diagram. An example of this type of sounding and distribu-
tion is shown in Figure 7b.

A large number of raindrop distributions have been
systematically observed in Oregon with raindrop cameras
(Mueller, 1962b). Film images of raindrops were then reduced
to average drop distributions for various rainfall rates and
synoptic conditions. These drop spectra were then fitted
with a curve of the form:

$$N_D = \alpha D^2 \exp(-\beta D^3) \qquad (2.0)$$

where the spatial distribution N_D is defined by fitting par-
ameters α and β for the diameters D to D + δ D. Table 3 sum-
marizes the parameters required to fit a number of average
distributions from Oregon under various synoptic conditions
and rainfall rates. Under low rainfall rates the curves
could be fitted by one set of α and β coefficients (fig. 8);
however, in heavier precipitation two curves were found neces-
sary to accurately fit the data (fig. 8 bottom). This dis-
tribution differs significantly from the MP (equation 1.1)
distribution and is used in experimentation with the Orville
model (see section 4 for detailed discussion).
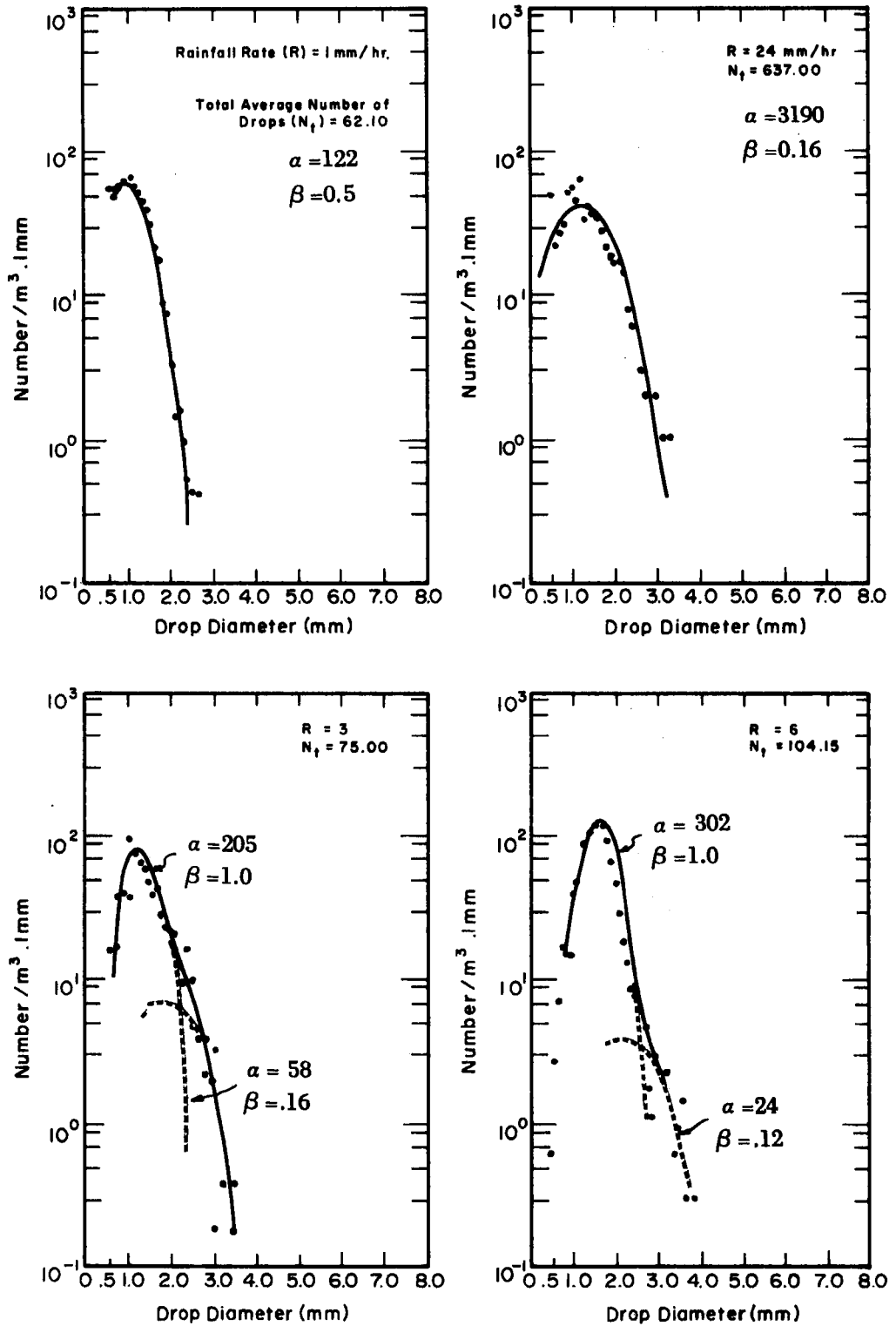
Fig. 8. Examples of curves fitting average distributions
from Oregon. Corresponding fitting parameters
(α , β) are shown with rainfall rates (R), and
total number of drops (N_T).

Other Mesoscale Raindrop Distributions

One of the most recent and comprehensive references of raindrop spectra was compiled by Fujiwara (1968). Fujiwara has described in detail the characteristics of drop distributions under various synoptic and climatological conditions. He has shown that the analysis of ISWS observations produce distributions which have larger widths and lower concentrations of the small size drops than that predicted by the MP distribution. For identical reflectivity and rainfall rates, the observed distributions and MP distributions are not always consistant. The average observed ISWS distribution was found to vary in total concentration, width of spectrum, skewness, and mode. For instance the droplet distribution from a weak rain shower, particularly of the orographic warm rain variety, is narrow and monomodal symetric. As rainfall intensity increased both the width and skewness increased. Fujiwara found that the maximum skewness occurs in the thunderstorm, when the distribution curve (N_D) becomes linear exponential; i.e. of the MP type.

Several different types of drop distributions have been related to the Z-R relation (equation 1.4) by Fujiwara. These distributions followed two basic patterns - monomodal and polymodal. Polymodal distributions tended to occur frequently in observations at large rainfall rates in

thunderstorms and rainshowers. Monomodal spectra were characteristic of low rainfall rates and steady rain. Figure 9 shows several cases which generally represent the thousands of observations made by the ISWS. The individual cases are shown on a general graph having ordinate of "a" and "b" as abscissa (a and b values are from the Z-R relation). For instance, monomodal distributions in the small "a" and "b" range (lower left of graph) occurred in steady rain on 26 October 1953 in rainfall water from .16 to 7.7 mm hr^{-1}. Skewed exponential distributions having polymodal spectra occurred in high values of "a" and medium values of "b" as illustrated by a thunderstorm on 3 July 1954; R = 16.3 to .16 mm hr^{-1}. In a case where strong wind shear occurred (10 October 1954) a polymodal skew distribution occurred suggesting that shear may tend to form polymodal distributions. The complexity of distributions observed by Fujiwara points to the fact that the exact physical processes which determine the complicated polymodal drop distributions may be difficult to describe.

Literature Summary

It is clear from numerous studies of raindrop size distribution that a large variety of raindrop spectra exists in nature. This variety of spectra changes depending upon the type of precipitation, rainfall rate, sounding properties, and geographical location. The dramatic
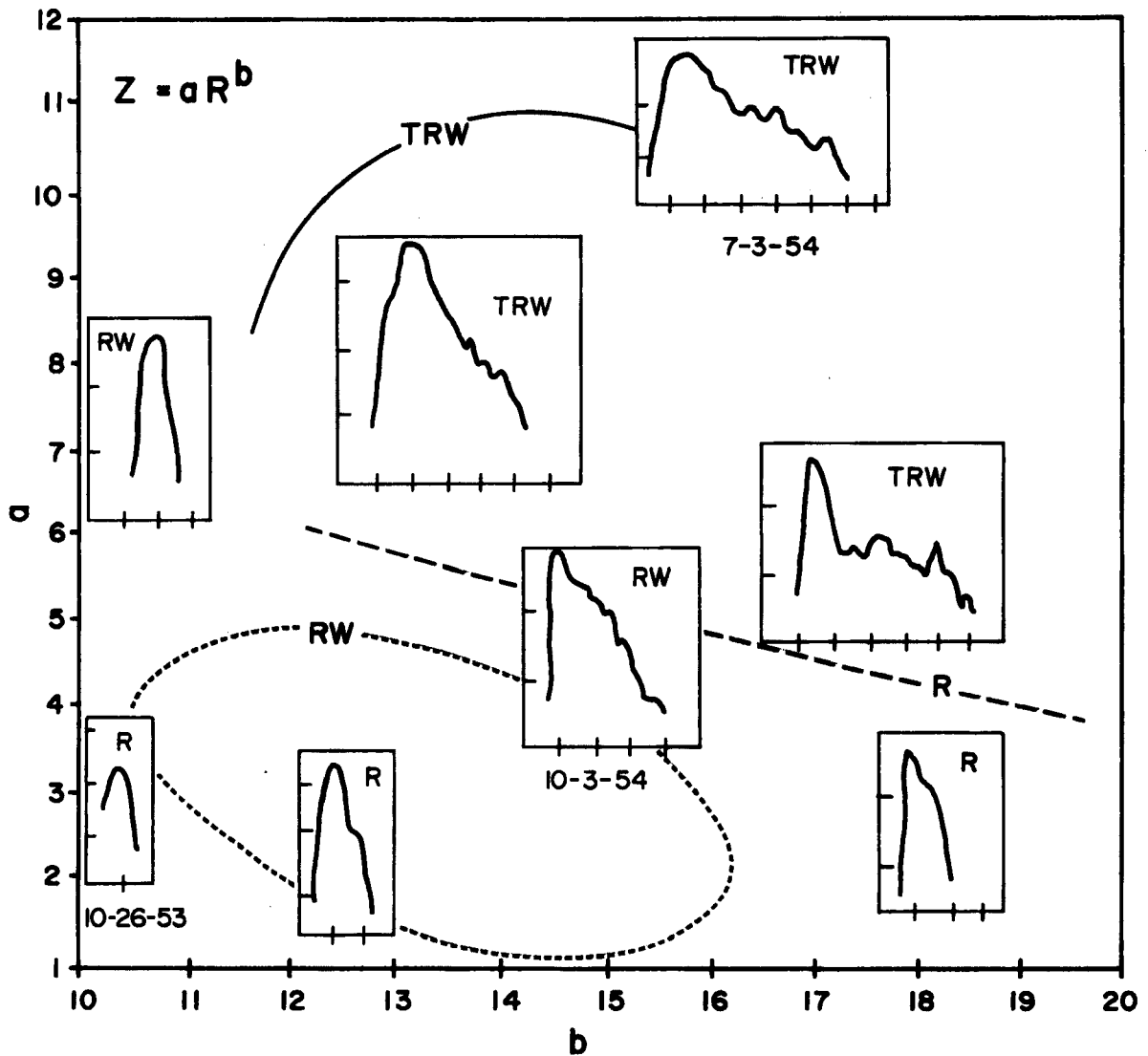
Fig. 9. Drop distributions for various precipitation types:
thunderstorm (TRW), rainshower (RW), continuous
rain (R*) plotted with corresponding a, b coef-
ficients of the Z-R relation (equation (1.4)).
The N_d spectra correspond to various rainfall
rates as shown in the upper-right corner of each
precipitation type and date (Fujiwara, 1968).

changes in drop spectra illustrate the need for better more explicit microphysical and parameterized modeling of raindrop size distributions.

The next sections will show how a change of raindrop spectra affects certain aspects of a cloud model which uses one drop spectra assumed by most cloud models today.

IV. SELECTION OF A REPRESENTATIVE DISTRIBUTION

An empirical size distribution of raindrops was needed to test a cloud model's sensitivity to changes in the form of an assumed raindrop spectra. One series of empirical drop spectra studies was selected as a basis from which one test set of spectra was then selected. This series of studies was made by the Illinois State Water Survey (Mueller, 1966) to improve point and aerial rainfall measurement as determined by radar observations. The sets of drop spectra obtained were observed by reasonably objective methods and their shape was reasonably consistant; therefore they appeared to be a reasonable facsimile of nature's drop spectra.

These sets of drop spectra met the following criteria: (1) provided a precise drop spectra based upon statistically significant sample sizes; (2) represented most major climatic types in which cloud models may be used; (3) could readily be utilized in cloud model calculations of hydrometeor growth. This section will elaborate further on the method by which ISWS collected and analyzed their data (Mueller, 1968).

Sample Size and Type

Sets of drop spectra were measured at seven stations around the world; these locations represented most moist

climatic types and indicated significant differences in characteristic drop spectra. The seven locations chosen were: Miami, Florida; Corvallis, Oregon; Majaro, Marshall Islands; Woodley Island, Alaska; Island Beach, New Jersey; and Franklin, N. C. These seven stations represent nearly all of the non-arid climatic regimes. Six hundred twenty-one days having rain were observed and a total of 20,380 one-minute samples of drop spectra were collected.

Camera Observation System

The raindrop camera used in the ISWS raindrop spectra sampling was designed and built by Mueller (1966). This camera is capable of measuring drops from 0.5 mm to 5.0 mm in a sampling volume of one cubic meter of air space. The camera samples one cubic meter per minute by making a series of seven frames per minute each covering a volume of .143 m^3. This sampling rate provided time to clear the sample volume of the previous sample. This technique produced a distribution of drop sizes per cubic meter per minute.

Raindrops could be resolved by the camera system to within ±0.2 mm (limited by the camera optics, film resolution, and "resetability" of calipers used in drop size measurement to the drop size image). Sizes from 0.5 mm to 5.0 mm in diameter could be measured. All drop distributions having less than 8 drops per m^3 were discarded because the sample size was too small to be representative of any significant rainfall amount.

The raindrop camera was set up on the ground in a clear area so that a representative raindrop sample could be taken. Exposure problems arose under conditions of high winds and very heavy rainfall rates because drops missed the sampling volume and water blurred the optics. In cases such as these the smaller drop sizes may not be counted due to: (1) their smaller terminal velocity, hence likelihood of being carried by the wind; and (2) their images being completely blurred out of focus by water splashed onto the optics.

In general, the measurement accuracy of drop images on film is the most uncertain due to the tedious nature of the sizing technique (caliper measurements). The precision of the number of drops in each category is within ±10% for drops 0.8 mm and larger in diameter. The number of drops with diameters between 0.5 and 0.8 mm were frequently found to be in greater error, however this did not effect the general spectra form at small sizes.

Drop Spectra Analysis

Due to the large variation in drops per size category of one minute samples, averages of samples were necessary to produce a representative drop spectra. These characteristic spectra were based on an average of one minute distributions representing the same rainfall rate. Mueller (1966) has shown that average spectra for the seven locations around

the world had rainfall rates from 1 mm hr^{-1} to 4.34 mm hr^{-1}. These distributions were monomodal, having modes between 0.9 and 2.0 mm. The distributions were fitted by a logarithmic function of the form:

$$N = \alpha D^2 e^{-\beta D^3} \qquad (2.0)$$

where α and β are empirical fitting parameters discussed further in section V. All general references to the ISWS drop spectra in this paper are to the distributions characteristic of various rainfall rates described by equation (2.0).

Characteristics of the Illinois State Water Survey Drop Spectra

The ISWS raindrop distributions obey an inverse exponential law having the form of equation (2.0). These spectra approach zero as diameter approaches zero and also as diameter increases beyond a critical median value, the number of drops per unit volume approaches zero.

The ISWS drop spectra differs from that of Marshall and Palmer in that they are parabolic spectra rather than linear when plotted on semi-log paper as illustrated by Figure 10. Here we see a linear distribution decreasing with large values of drop diameter as expected by equation (1.1) for the MP spectra. In contrast, the ISWS
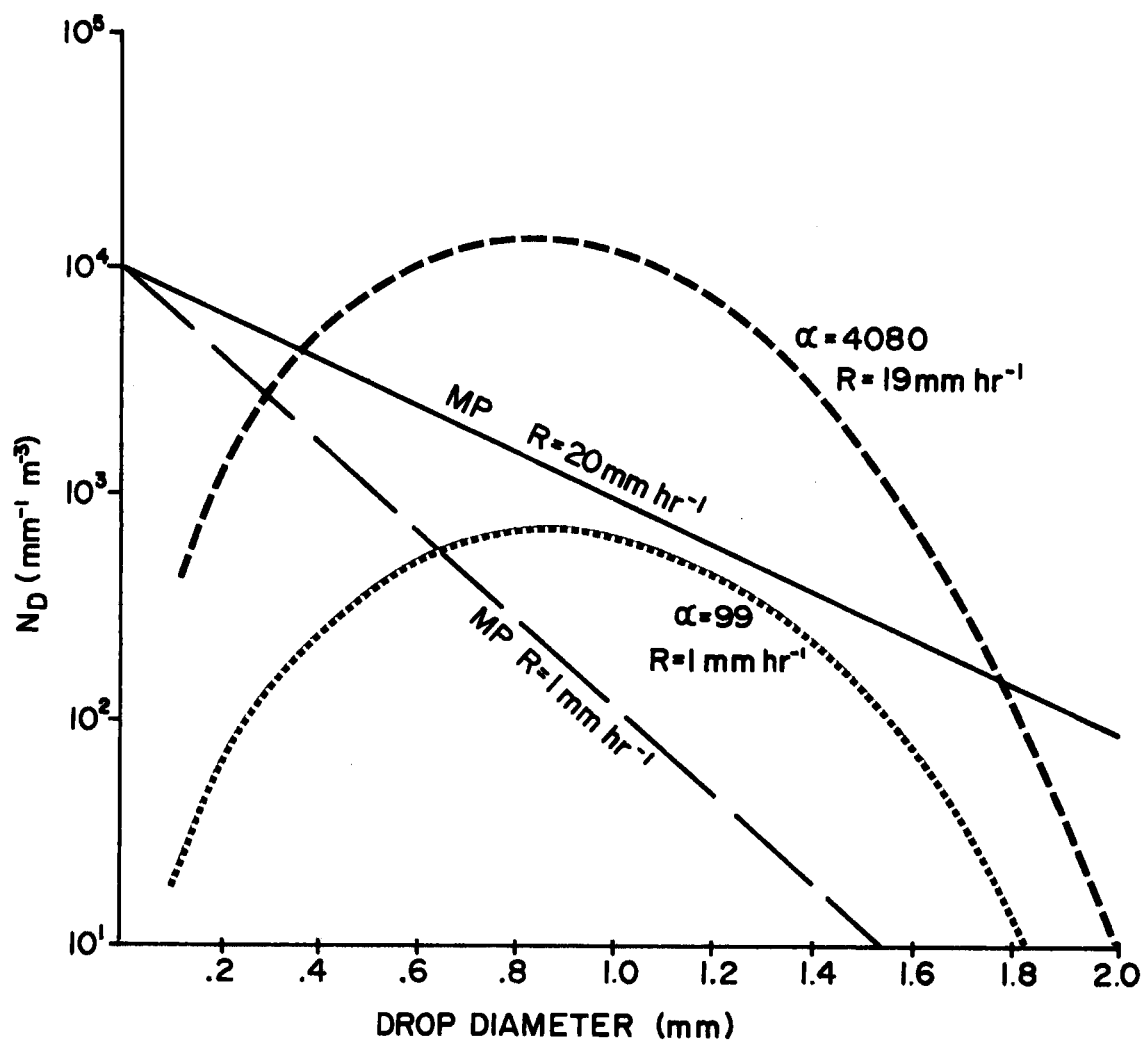
Fig. 10. A comparison of MP and ISWS spectra. ISWS distributions are defined by their corresponding α coefficients of 4080 and 99.

distribution equation (2.0) is also exponential in D; however, on semi-log paper it is parabolically approaching zero at both small and large drop diameters. This limited spectra would be expected in nature due to the following four processes:

    (1)   break up of large drops into smaller ones caused by drop surface instabilities (Blanchard, 1948);

    (2)   coagulation of drops;

    (3)   accretion of smaller drops by larger drops (Hardy, 1965);

    (4)   and evaporation of very small drops.

One representative set of ISWS spectra was selected from the seven sets representing most moist climates. The set of raindrop spectra observed in Oregon was selected because it generally represented the form of spectra in the other six regions and showed spectra variations with respect to synoptic conditions and rainfall rates. Three individual Oregon spectra were then compared with the MP spectra in the Orville symmetric cloud model. These three spectra represented three different synoptic types (air mass, cold frontal and "post warm frontal occlusion-orographic") and rainfall rates of 1, 2 and 19 mm hr^{-1}, respectively.

Detailed analysis of the mass distributions for Oregon rainfall spectra (Table 4) shows a large range of concentration for various precipitation rates of the first ten

synoptic types of Table 3. The precipitation water content
contributed by each diameter category undergoes considerable
change with drop size. Detailed 0.1 mm computations with
this mass spectra show a shift of mode mass from .3 to .9 mm
diameter with an average range of peak mass diameter of .5
mm. This shift corresponds to a terminal velocity change of
2.0 to 4.0 mps, an increase of 40 to 80% of the original
median value terminal velocity of the drop size spectra.
An increase of this magnitude is significant in considera-
tions of cumulus dynamics within cloud models; however, in
the real atmosphere temporal and spatial variations on this
order are not uncommon (Lhermitte, 1966).

Statistical analysis of the set of Oregon spectra re-
veals rather large standard deviations of the drop spectra
in each size category. Table 5 presents the range and
average concentrations of selected drop categories. For a
case of 24 mm hr^{-1}, rainfall in overrunning orographic con-
ditions we have a maximum concentration of 4240 drops per m
at the 1.6 mm diameter whereas with a rainfall rate of 6 mm
hr^{-1} and warm frontal orographic conditions 3×10^{-8} drops per
m were observed with a 2.0 diameter. Examples of extremes
are illustrated in Table 5 for selected drop categories.
Largest standard deviations are observed in drop sizes which
contribute significantly to the precipitation water content.

Table 3

Regression Coefficients From Oregon Data

* = Two curves necessary - mode location refers to first coalescence curve.
\# = No fit possible with curves.
1 = Coefficients used in Orville cloud model experiment (section V).

Rain Rate R (mm/hr)	Regression Coefficients α	β	Maximum N_D (no./m^{3}mm)	Mode Location D (mm)	Synoptic Type	Synoptic Type Code
1	242	1.00	95	0.85	Air Mass	(1)
3	154	.50	76	1.10	Air Mass	
6	99	.30	86	1.30	Air Mass	(1)
9	#	-	-	-	Air Mass	
1	184	1.00	72	.91	Air Mass Orographic	
2	294	1.00	117	1.15	Air Mass Orographic	
6	500	1.00	200	1.32	Air Mass Orographic	(2)
8	#	-	-	-	Air Mass Orographic	
1	#	-	-	-	Cold Frontal	
2	440[1]	1.00	180	.90	Cold Frontal	(3)
1	#	-	-	-	Post Cold Frontal	
2	400	.50	200	.80	Post Cold Frontal	(4)
6	1560	1.00	620	.95	Post Cold Frontal	
1	136	1.00	54	1.15	Post Cold Frontal Orographic	
3	249	1.00	96	1.10*	Post Cold Frontal Orographic	
6	400	1.00	160	1.20*	Post Cold Frontal Orographic	(5)
8	755	1.00	305	1.10*	Post Cold Frontal Orographic	
14	3700	1.20	1250	1.09	Post Cold Frontal Orographic	
1	122	.50	62	.90	Overrunning Orographic	
2	249	.50	125	1.00	Overrunning Orographic	
6	329	.50	161	1.20*	Overrunning Orographic	
8	440	.50	220	1.25*	Overrunning Orographic	(6)

Table 3 (Cont'd)

Rain Rate R (mm/hr)	Regression Coefficients		Maximum N_D (no./m³ mm)	Mode Location D (mm)	Synoptic Type	Synoptic Type Code
	α	β				
12	1590	1.20	550	1.05*	Overrunning Orographic	
24	3190	.16	415	1.18	Overrunning Orographic	
26	590	.30	520	1.25	Overrunning Orographic	
1	1000	3.00	190	1.25	Warm Front	
3	740	2.00	180	1.20	Warm Front	(7)
6	790	1.00	335	1.20	Warm Front	
1	128	1.00	52	1.15	Warm Frontal Orographic	
3	205	1.00	82	1.15*	Warm Frontal Orographic	
6	560	3.00	148	1.10*	Warm Frontal Orographic	(8)
9	2200	1.20	760	1.06*	Warm Frontal Orographic	
13	1970	1.20	680	1.15*	Warm Frontal Orographic	
1	258	1.20	90	1.00	Warm Occlusion Concurrent	(9)
1	130	1.00	52	.93*	Warm Occlusion Orographic	
3	245	1.00	100	1.24	Warm Occlusion Orographic	
6	302	1.00	120	1.60*	Warm Occlusion Orographic	(10)
10	400	1.00	160	1.60	Warm Occlusion Orographic	
12	460	1.00	220	1.65	Warm Occlusion Orographic	
24	#	-	-	-	Warm Occlusion Orographic	
1	277	1.20	96	1.05	Pre-Warm Occlusion	
2	179	1.00	72	1.25	Pre-Warm Occlusion	(11)
6	150	.50	76	1.55	Pre-Warm Occlusion	
8	#	-	-	-	Pre-Warm Occlusion	
1	125	.50	57	.90	Pre-Warm Occlusion Orographic	
2	409	1.20	146	1.25	Pre-Warm Occlusion Orographic	(12)

45

Table 4

Illinois Water Survey Drop Distribution Statistics

Mass Per Size Category

Oregon Data 1962

			Diameter: .5 mm		1.0 mm		2.0 mm		Peak	
Case	Rainfall Rate		Concen- tration No m^{-3}	Total Mass (gm m^{-3})	Concen- tration (No m^{-3})	Total Mass (gm m^{-3})	Concen- tration (No m^{-3})	Total Mass (gm m^{-3})	Diameter (mm)	Concen- tration No m^{-3}
1	1.0	1*	53.4	.0279	89.0	.372	.325	.010	.9	94.6
2	3.0		36.2	.0195	93.4	.391	11.3	.378	1.1	95.8
3	6.0		23.8	.0124	73.3	.307	35.9	1.202	1.3	86.6
4	1.0	2	40.6	.0212	67.7	.283	.247	.0082	.9	71.9
5	2.0		64.9	.0339	108.	.452	.395	.013	.9	115.
6	6.0		110.0	.0575	184.0	.770	.671	.011	.9	195.
7	2.0	3	97.1	.050	162.0	.678	.590	.019	.9	172.
8	2.0	4	93.9	.049	243.	1.017	29.0	.971	1.1	249.
9	6.0		344.0	.180	574.	2.404	2.09	.070	.9	610.
10	1.0	5	30.0	.015	50.0	.209	.182	.006	.9	53.1
11	3.0		54.9	.028	91.6	.383	.334	.011	.9	97.3
12	6.0		88.2	.046	147.	.615	.537	.017	.9	156.0
13	8.0		167.	.087	278.	1.164	1.01	.033	.9	195.0
14	14.0		796.	.416	1110.	4.649	1.00	.033	.8	1280.0

46

Table 4 (Continued)

Illinois Water Survey Drop Distribution Statistics

Mass Per Size Category

Oregon Data 1962

Diameter:			.5 mm		1.0 mm		2.0 mm		Peak	
Case	Rainfall Rate		Concen-tration No m^{-3}	Total Mass (gm m^{-3})	Concen-tration (No m^{-3})	Total Mass (gm m^{-3})	Concen-tration (No m^{-3})	Total Mass (gm m^{-3})	Diameter (mm)	Concen-tration No m^{-3}
15	1.0	6*	28.7	.01	74.0	.30	8.94	.299	1.1	75.9
16	2.0		58.5	.03	151.0	.63	18.2	.60	1.1	155.
17	6.0		77.3	.04	200.0	.83	24.1	.80	1.1	205.
18	8.0		103.0	.05	267.0	1.11	32.0	1.07	1.1	274.
19	12.0		342.0	.18	479.0	2.00	.431	.014	0.8	550.
20	24.0		782.0	.41	2720.0	11.3	3550.0	118.9	1.6	4240.
21	26.0		142.0	.07	437.0	1.83	214.	7.1	1.3	516.
22	1.0	7	172.0	.09	49.8	.21	.151 E-06	.10^{-8}	0.6	188.
23	3.0		144.	.07	100.	.41	.33 E-03	.10^{-5}	0.7	183.
24	6.		174.	.09	291.	1.22	1.06	.03	0.9	309.
25	1.0	8	28.0	.01	47.0	.19	.172	.17	0.9	50.0
26	3.0		45.2	.02	75.4	.31	.275	.01	0.9	80.0
27	6.0		96.2	.05	27.9	.11	.84 E-07	.10^{-8}	0.6	105.0
28	9.0		473.	.24	663.	2.78	.596	.59	0.8	762.0
29	13.0		424.	.22	593.	2.48	.534	.07	0.8	682.0
30	1.0	9	55.5	.02	77.7	.32	.069	.002	0.8	89.3
31	1.0	10	28.7	.01	47.8	.20	.005	.005	0 0	50.8

* Synoptic Type

47

Table 5

Statistical Summary of Oregon Data

CONCENTRATIONS (No/m^{-3})

Radius mm	Maximum	Minimum	Mean	Standard Deviation	Total Number of Drops Observed
.1	40.7	.98	6.7	4.8	337.
.2	161.6	3.9	26.8	19.1	1340.
.5	877.0	36.0	147.8	103.2	7390.
1.0	2718.0	30.	258.7	137.2	12936.
1.5	4182.	10.	140.2	2.7	7011.
2.0	3547.	$3.0x10^{-8}$	79.6	11.1	3983.

V. ANALYSIS OF DROP SPECTRA EFFECTS ON A CLOUD MODEL

Selection of Model in Which to Test Hypothesis

In order to test the hypothesis that different raindrop spectra can significantly affect the empirical modeling methods for rain and cloud water determination in convective cloud models, a model must be used which has somewhat realistic precipitation processes. The model must be capable of describing the growth of a convective cloud in two dimensions (x, z) and be time dependant to produce a close approximation of nature. For purposes of comparison the model must utilize an empirical parameterized cloud microphysics based upon Kessler's (1969) parameterization. Use of Kessler's parameterized microphysics is important because it is currently the foundation for a number of widely used cloud models: Murray (1970); Orville (1969); Weinstein-Davis (1968); Simpson and Wiggert (1969); and others. An empirical system of cloud microphysics rather than one based on first principles is necessary in today's models due to the limitations of both time and space imposed by today's hardware. Numerical solution of both detailed cloud microphysics and dynamics is not yet possible on currently available hardware. Thus cloud models today rely upon the fast and economical parametric microphysics.

To determine the effects of rain distributions on cloud growth the solutions of the hydrodynamic equation of motion governing cloud dynamics must include the direct effects of water loading which is the net "drag" of falling raindrops on cloud updrafts. Distributions of both rainwater and cloud water must be capable of interacting with cloud dynamics. Modeled cloud microphysics should include effects of evaporation of drops, autoconversion from cloud to rainwater, and accretion of cloud droplets by raindrops.

One model which meets all of the above criteria is the Orville Symmetric Cloud Model (Orville, 1965, 1969). This is a two dimensional time dependant cloud model which numerically integrates the equations of motion, equations of conservation of water substance, and thermodynamic energy equations at 200 meter grid point intervals on a 50 by 50 point grid (see fig. 11). Initial development of convection and evaporation are simulated by a solar heating function which simulates surface heating on a mountain at the center of the surface boundary (see fig. 11) and a flux of moisture through this boundary (see Orville, 1969).

The model is based on the following assumptions (Orville, 1969):

(1) The cloud is two dimensional in the x-z plane.

(2) The air flow is non-divergent, thus enabling stream function calculations.
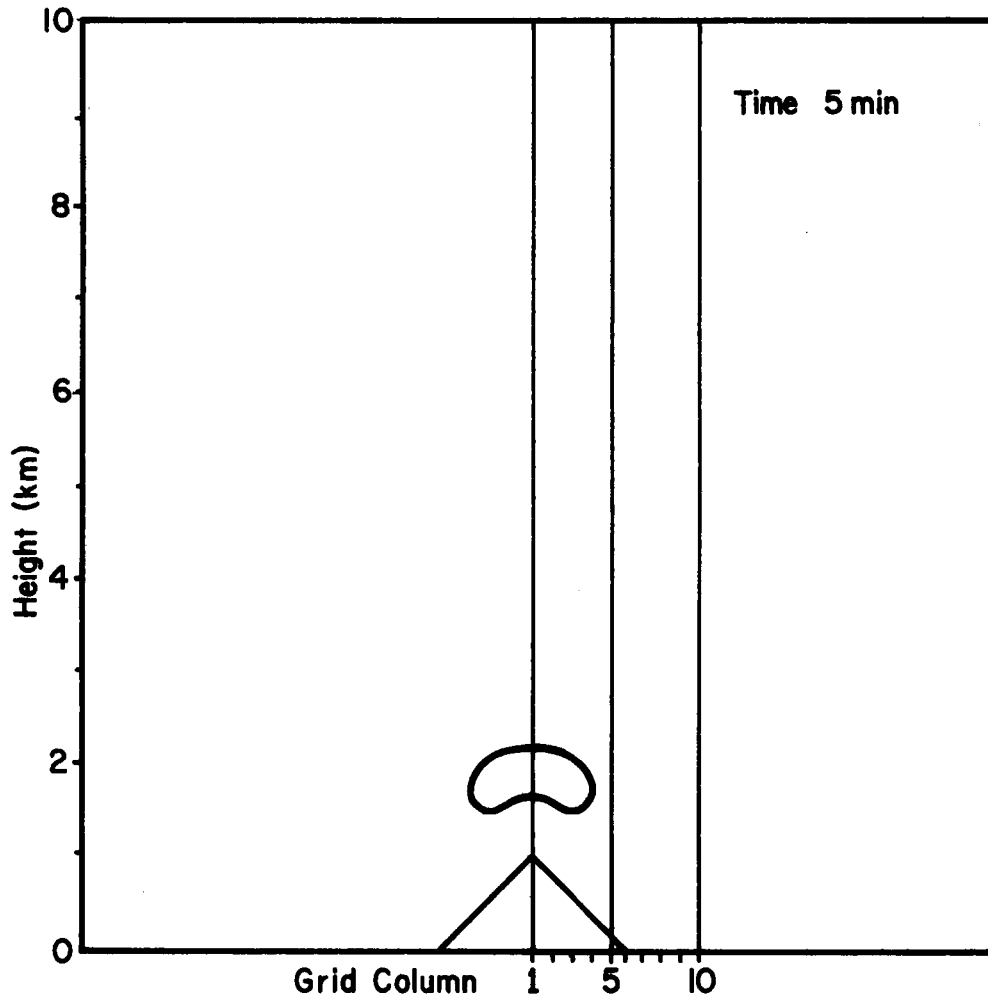
Fig. 11. Cloud model grid showing vertical and horizontal
scales. Vertical and horizontal grid points are
200 meters apart on a 50 by 50 point grid. The
central grid column is identified as 1, and column
numbers increase toward the right (left side is
symmetric to right side). Initial cloud outline
after 5 minutes of growth is shown.

(3) The eddy diffusion coefficients for heat, momentum, cloud water and water vapor are constant.

(4) Any excess water vapor over that required to saturate the air condenses to cloud water immediately. Likewise a deficit below saturation in cloud is immediately supplied by evaporation of cloud water.

(5) The raindrop distribution is an exponential function of diameter based on the Marshall-Palmer spectra (1948).

(6) Raindrops are always at their terminal velocity relative to ambient air.

(7) Cloud water conversion to rainwater is parameterized after Kessler (1969).

(8) The collection efficiency is set at 1.0 throughout the accretion process.

(9) Electrical effects, freezing processes, and the Coriolis forces are neglected.

(10) Cloud water and water vapor are conserved in the parcel; however, rainwater falls out.

Continuity of water substance is achieved by a balance between water vapor convergence, cloud water convergence and rainwater convergence. The following section describes in detail the hydrometeor growth equations used by the model.

Hydrometeor Growth Equation

Most cloud models use the general hydrometeor growth equation (2) to compute the development of precipitation. Two derivations of the hydrometeor growth equation are presented in this section; one assumes a MP spectra, the

other an ISWS spectra. These derivations are shown for both
a one dimensional steady state cumulus model (Weinstein,
1967), and a two dimensional time dependant cumulus model
(Orville, 1969). The resulting relations shown by equations
(6) and (10) for the Weinstein model, and (15) and (17) for
the Orville model illustrate the differences between MP and
ISWS spectra in hydrometeor growth equations.

If one defines hydrometeors as rain droplets of 100 μ
diameter or greater one can then apply the continuous collec-
tion process for growth described by Langmuir (1948). The
growth of an individual droplet by sweeping out a volume
of $\frac{\pi D^2 V}{4}$ is:

$$\frac{\delta m}{\delta t} = \frac{\pi D^2}{4} VEQ_c \rho_a$$

where V is the terminal velocity of drop, E is the collection
efficiency, Q_c is the cloud liquid water content, and ρ_a
is the density of air. Thus the growth equation for all
hydrometeor water is an integration over-all drop sizes:

$$\frac{dQ_h}{dt} = \frac{1}{\rho_a} \int_0^\infty \frac{\delta m}{\delta t} N\delta D$$

where N is the drop spectra per unit volume as defined by a
given precipitation distribution.

Most models which use an empirical microphysics approach
assume a Marshall-Palmer distribution:

$$N = No \exp (-\lambda D) \qquad (3)$$

where N is the number of drops having a diameter between D and D+ δD, No is the number of drops of diameter D=0, where No=0.08 cm. (Number/m.$^{-4}$) and λ =41R$^{-.21}$ where R is the rainfall rate in mm hr^{-1}.

Substitution of (1) and (3) into (2) gives a general form of the hydrometeor growth equation.

$$\frac{dQ_h}{dt} = \frac{\pi}{4} \ E \ \cdot \Omega_c \int_0^\infty V \ D^2 \ No \ exp(-\lambda D) \delta D \tag{4}$$

When we assume a terminal velocity of the form (Kessler, 1970):

$$V = 130 \ D^{1/2} \tag{5}$$

we then have:

$$\frac{dQ_h}{dt} = \frac{130^\pi}{4} \ E \ Q_c \ No \int_0^\infty D^{2.5} \ e^{-\lambda D} \ dD \tag{6}$$

where E is assumed independent of diameter D.

Solving this integral using a gamma function, we have:

$$\frac{dQ_h}{dt} = 32.5 \ E \ Q_c \ No \ \Gamma \ (3.5)/ \ \lambda^{3.5} \tag{7}$$

The above hydrometeor growth relation is used in the Weinstein (1968) one-dimensional steady state and time dependent models.

Assuming a more flexible precipitation spectrum such as that of the Illinois State Water Survey:

$$N = \alpha \int D^2 \ exp(-\beta D^3) \delta D \tag{8}$$

where N is the number of drops found between D and D+δD, α and β are curve fitting coefficients and D the diameter of the particles in mm. Using this relationship in equation (2), we have:

$$\frac{dQ_h}{dt} = \frac{\pi}{4} \ E \ Q_c \alpha \int V \ D^4 \ \exp(-\beta D^3) \ \delta D \qquad (9)$$

or in terms of Kessler's terminal velocity used in the Weinstein models (1967, 1968):

$$\frac{dQ_h}{dt} = \frac{130\pi}{4} \ E \ Q_c \ \alpha \int D^{4.5} \ \exp(-\beta D^3) \ \delta D \qquad (10)$$

which reduces on integration over-all diameters to a gamma function solution:

$$\frac{dQ_h}{dt} = \frac{130\pi}{4} \ \alpha \ Q_c \ E \ \Gamma(1.83)/\beta^{1.83} \qquad (11)$$

The hydrometeor growth relation utilized by the Orville symmetric cloud model is basically the same as equation (2), however Orville (1969) uses a different terminal velocity:

$$V_d = a(D/D_r)^b \qquad (12)$$

where D_r is a reference diameter (1 cm.) and constants a and b are 2115 cm. sec.$^{-1}$ and 0.8 respectively. This relation was based on thirty pairs of terminal velocities and diameters of raindrops selected from the Smithsonian Meteorological Tables (List, 1958) and fitted by the

least-square method.

Substituting this terminal velocity (12) into the growth equation (2), we have:

$$\frac{dQ_h}{dt} = \frac{E \rho Q \pi}{4} \ a \int_o^\infty D^2 \ (\frac{D}{D_r})^b \ N \ \delta D \qquad (13)$$

Assuming a Marshall-Palmer precipitation spectra (3) we now have:

$$\frac{dQ_h}{dt} = E_c \ \rho \ Q_c \ \frac{\pi}{4} \ a \ No \int_o^\infty \left(\frac{D}{D_r}\right)^b \ \exp(-\lambda D) \ \delta D \qquad (14)$$

which reduces to a gamma function solution of the form:

$$\frac{dQ_h}{dt} = \frac{\pi \ \rho \ Q_c \ E_c \ No \ a}{4 \ D_r^b} \int_o^\infty D^{(2+b)} \ \exp(-\lambda D) \ dD \qquad (15)$$

upon integration, we have:

$$\frac{dQ_h}{dt} = \frac{\pi \ \rho \ \Omega_c \ E_c \ No \ a}{4 \ D_r^b} \ \Gamma(3+b)/\lambda^{3+b} \qquad (16)$$

where E_c is assumed equal to 1. Orville (1969) has shown that this result is 10% smaller than that of Kessler (1969) at $Q_c = Q_h = 1$ gm. m^{-3}.

When we substitute the Illinois State Water Survey spectra (8) into equation (12), we have:

$$\frac{dQ_h}{dt} = \frac{\pi \ \rho \ Q_c \ E_c \ \alpha a}{4} \int D^4 \left(\frac{D}{D_r}\right)^b \exp(-\beta D^3) \ dD \qquad (17)$$

which reduces to

$$\frac{dQ_h}{dt} = \frac{\pi \ \rho \ Q_c \ E_c \ \alpha \ a}{4 \ D_r^b} \int D^{4+b} \ \exp(-\beta D^3) \ dD \qquad (18)$$

upon integration, we have:

$$\frac{dQ_h}{dt} = \frac{\pi \rho Q_c E_c \alpha a}{12 D_r^b} \Gamma \frac{(5+b)}{3} \bigg/ \beta \frac{5+b}{3} \quad (19)$$

Analysis of the ISWS Oregon drop spectra of Table 5 reveals a large variation in the peak of drop distributions which could significantly affect the rate of hydrometeor growth shown in equation 1. The location of the mode of the distributions varies from .80 to 1.65 mm. This shift in mode changes the median volume terminal velocity as much as three meters per second when using Kessler's (1969) relation for terminal velocity:

$$V_T = -130 \ D^3$$

where V_T is the terminal velocity in meters per second and D is drop diameter in meters.

A variation of three meters per second in terminal velocity could have significant effects on cloud modeling results because it changes the distribution of water throughout the cloud due to cloud dynamics and plays an important role in microphysical processes of collection, see equation (1). The wide range of concentrations of large drops is also an important factor in the calculations for water loading, duration of precipitation, onset time of precipitation, and microphysical collection and hydrometeor growth.

Experimental Procedure

Four comparative experiments with the Orville symmetric cloud model were made using the hydrometeor growth relation assuming an MP distribution (16) and an ISWS distribution (19). For comparative purposes all conditions within the model were identical with the exception of the type of raindrop distribution assumed in the hydrometeor growth equation. Three ISWS spectra were used in the experiment corresponding to values of the three fitting coefficients of equation 8 given in Table 4. Alpha values corresponded to the maximum 4080, minimum 99, and an average of 440. Results using the 440 value of α will not be discussed in this paper because they fall between those of the maximum and minimum and add little additional information.

The particular sounding of temperature and dewpoint assumed in the model experiment is shown in Figure 12. The lapse rate of potential temperature was 2.8 °K/km from the surface up to 8 km above which it was 10 °K/km. At the surface the mixing ratio was assumed 10 gm/kgm and decreased at a rate of 2 gm/kgm per km.
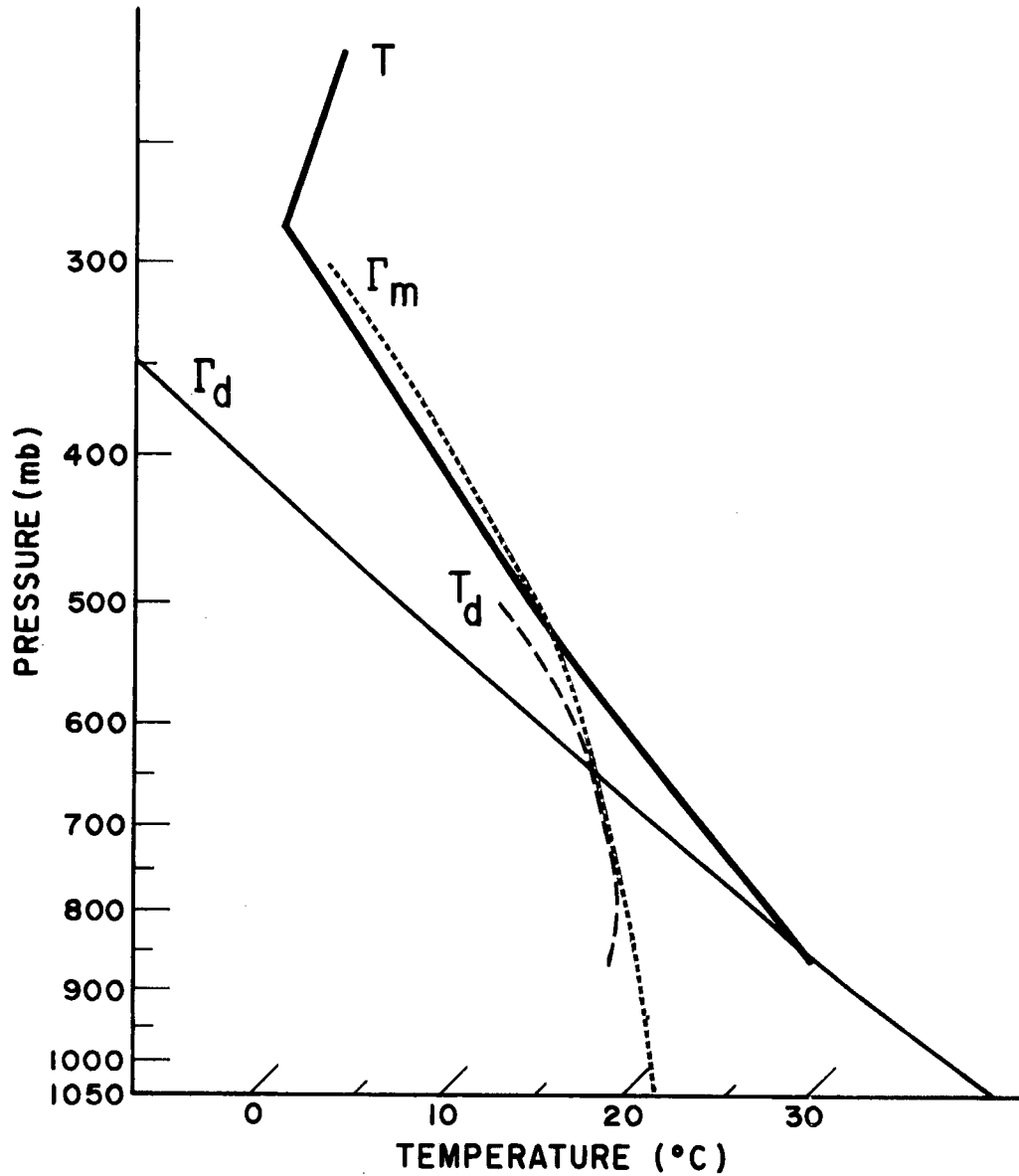
Fig. 12.   Sounding used in Orville Symmetric Model experi-
ment is illustrated in relation to the moist (Γ_m)
and dry (Γ_d) adiabatic lapse rates.   T   is the
temperature and T_d is the dewpoint of the
sounding.

VI. ORVILLE SYMMETRIC CLOUD MODEL RESULTS

Three experiments were performed using different drop spectra in the Orville symmetric cloud model. Different values of rain and cloud water developed in the cloud when the three spectra were used. These changes were analyzed in terms of vertical profiles of liquid water content for rain and cloud water throughout the cloud. Each vertical profile consisted of all grid values for a column through the cloud from the surface to 10 km. The grid used in the cloud model is shown in Figure 11. Grid columns are at 200 meter intervals and are labled from the center (mountain peak, grid 1) to the grid boundary (grid 24). The mountain boundary extends from the central grid 1 to grid 6 and has a height of 1.0 km.

There were noticeable departures from the values of rain and cloud water obtained using the Marshall-Palmer spectra. These departures appear to be significant because they are above the model "noise levels" of cloud and rainwater.

Cloud Water Profiles

In general the cloud water content was greater using the ISWS spectra than using the MP spectra. As the cloud developed, the cloud water content increased to 30-40% more

than that of the MP case. Initially the differences were less than 5%; however, after 10 minutes of cloud development increases on the order of 15-30% were observed at various grid points in the cloud. After 33 minutes of cloud growth, the differences were on the order of 50-100% more than MP. Two coefficients were used for α in equation (8), 99 and 4080, which correspond to rainfall rates of 6 and 19 mm hr^{-1}, respectively. As the cloud develops in time, the variation between the spectra for the two α values tends to increase from less than 1% difference to values of 40-60% throughout the cloud.

Examples of Spectra Effects on Cloud Water

One example of the shift in cloud water from that developed by MP distribution to that developed by the ISWS distribution is illustrated by Figure 13a. Here, after 12 minutes of cloud development on grid column 1, we see that using a coefficient of $\alpha = 4080$, we have a distinct increase in cloud water below 2.8 km and very little change in cloud water above this level. The cloud water generated using an α of 99 produced a profile nearly identical to that of MP. A significant increase in the cloud water below the MP cloud base is characteristic of the ISWS profiles. This increase probably is due to an increase in the drop sizes and number of drops at the base of the cloud. Thus evaporation does not dissipate the cloud as easily as with the standard MP precipitation spectra.
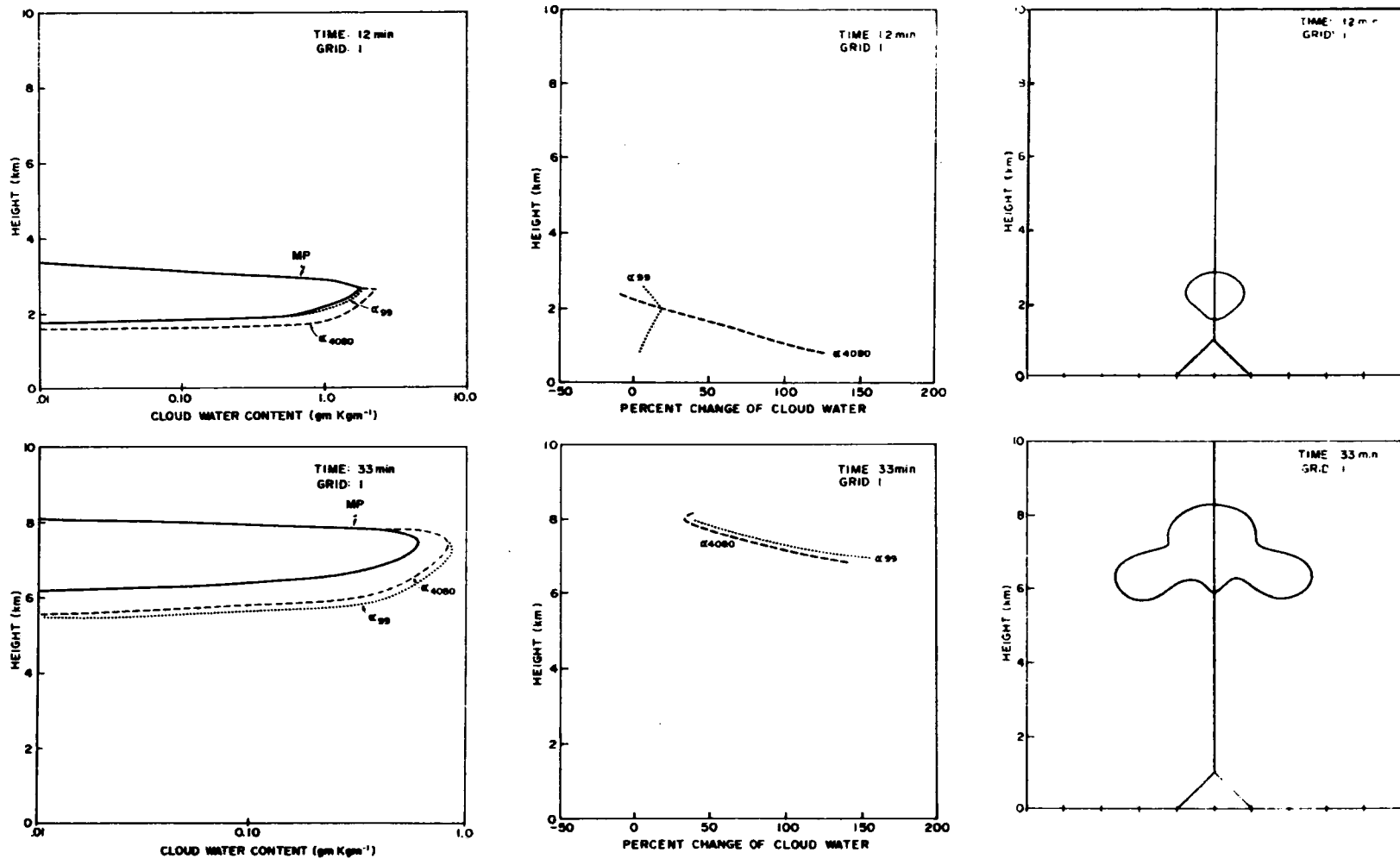
TIME: 12 min
GRID: I

HEIGHT (km)

MP

α 99
α 4080

CLOUD WATER CONTENT (gm Kgm⁻¹)

TIME: 12 min
GRID: I

HEIGHT (km)

α 99
α 4080

PERCENT CHANGE OF CLOUD WATER

TIME: 12 m r
GRID: I

HEIGHT (km)

TIME: 33 min
GRID: I

HEIGHT (km)

MP

α 4080
α 99

CLOUD WATER CONTENT (gm Kgm⁻¹)

TIME: 33min
GRID: I

HEIGHT (km)

α 4080
α 99

PERCENT CHANGE OF CLOUD WATER

TIME: 33 m.n
GRID: I

HEIGHT (km)

Fig. 13.   Vertical Profiles of Cloud Water Content (a) and Percentage Changes of
ISWS Case From MP Case (b) Together With Corresponding Cloud Outlines
(c) at 12 and 30 Minutes of Cloud Growth.   MP and Two ISWS Profiles
Corresponding to α 99 and α 4080 Are Shown in Figure.

Looking at the percent difference profile (fig. 13b), one can see a relatively small difference between the α99 and the MP profile. This departure from the MP cloud is small at the cloud top (only 2-5%) and larger at mid-cloud (10-20%). The α4080 profile was distinctly different from the MP case having differences from 130% at cloud base to -5% at cloud top. Figure 13c shows the cloud outline with respect to the mountain peak and computer grid. The vertical line above the mountain peak shows the location of the vertical profile through the cloud.

As the cloud develops, the departure from the MP cloud water becomes more significant because larger amounts of liquid water are present during the later stages of development. One example of the cloud water differences that occur later in development occurred after 33 minutes of cloud growth. Grid column 1 in Figure 13b shows a cloud top which is 30% greater than that of the MP case increasing to 155% greater for $\alpha = 99$ and over 145% for $\alpha = 4080$ at mid-cloud levels. The level of the cloud base is shifted three grid levels (600 m) lower. The bulk of the cloud has liquid water contents on the order of 0.3-0.5 gm kgm^{-1} using the MP distribution, whereas for the ISWS we have a significant increase to 0.5-0.8 gm kgm^{-1} .

Examination of the rainwater in the next section shows
that these cloud water contents are consistent with the
values of rainwater content from 0.4-2.9 gm kgm^{-1} for MP
and 0.4-4.2 gm kgm^{-1} for ISWS.

Rainwater Profiles

Early in cloud development we see that there are
distinct effects of the ISWS spectra on hydrometeor water.
Both coefficients of α produce markedly different precipita-
tion profiles in contrast to very similar profiles of cloud
water. The smaller α value of 99 produces a smaller amount
of hydrometeor water throughout the lower regions of the
cloud initially as in Figures 14 for 12 minutes of cloud
growth at grid 1. Whereas the larger value of α = 4080
produced a smaller amount of rainwater at cloud top than MP;
however, toward cloud base it produced more rainwater than
the MP cloud (fig. 14a). At this stage, the rainwater con-
tent for the MP distribution lies between .2 and .45 gm kgm^{-1},
whereas the smaller α coefficient produced rainwater con-
tents from .12 to .32 gm kgm^{-1} and the larger α coefficient
produced values from .18 to .43 gm kgm. The percentage
change of these values from the MP case (fig. 14b) shows
that the ISWS rainwater content was 40% below that of the
MP case near cloud top and increased toward the MP value
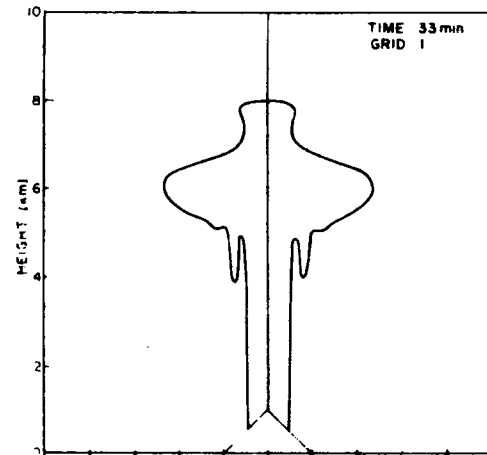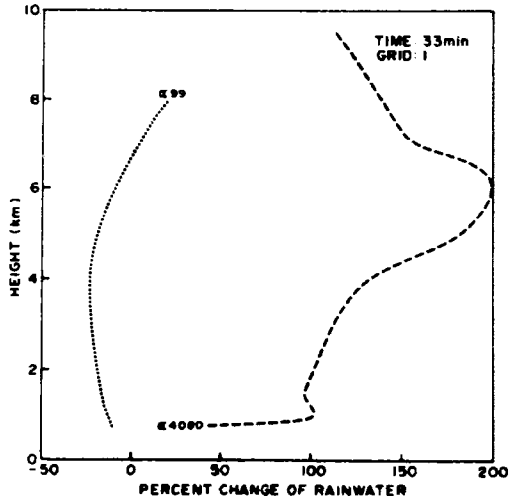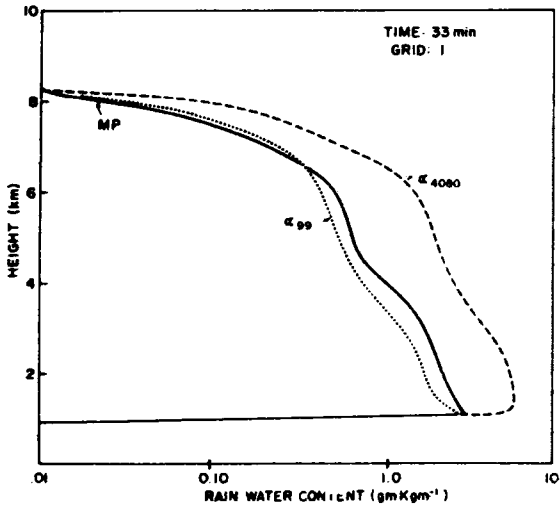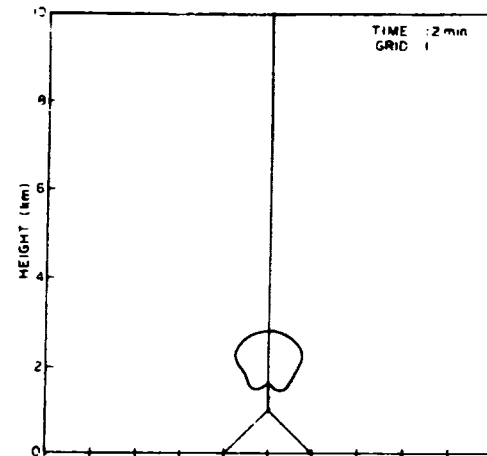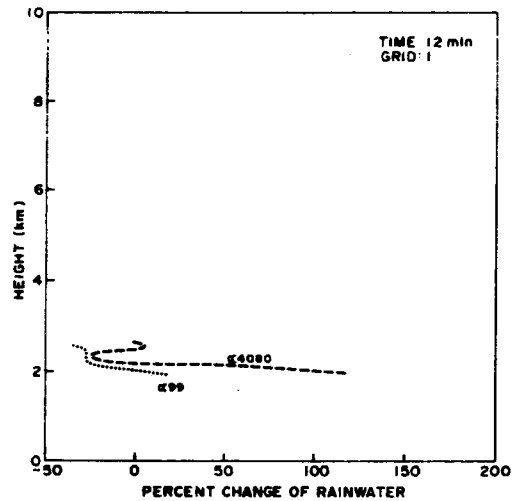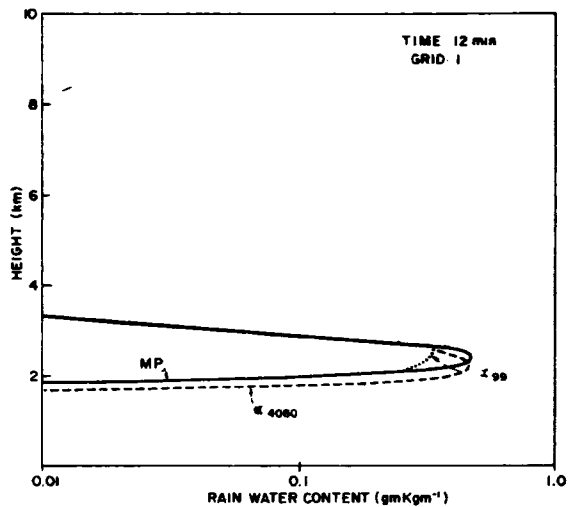lower in the cloud. Near cloud and precipitation base the

Fig. 14. Vertical Profiles of Rainwater Content (a) and Percentage Change of ISWS Case From MP Case (b) Together With Corresponding Cloud Outlines (c) at 12 and 30 Minutes of Cloud Growth. MP and ISWS Profiles as in Figure 13 are Shown.

small α ISWS case was within 5% of the MP values; however the large α ISWS case departed from the MP case by more than 120% near precipitation base. There is an important shift of precipitation to lower levels in the cloud. This shift may be due to greater rainwater content which through microphysical parameterization would produce a larger median raindrop diameter which would have a greater terminal velocity. These larger particles would then fall out more readily.

During later stages of cloud development there is a more distinctive change in the ISWS rainwater profiles. After 33 minutes of cloud growth in column 1 (fig. 14a), we have a significant increase in rainwater above 7.0 km for the large α case. Whereas the small α profile is greater than the MP profile from cloud top to 7.0 km then is below the MP profile to cloud base. The large α profile is distinctly greater than MP throughout the cloud. The profiles in figure 14 show the increasing departure of the ISWS profiles from that of MP as time increases.

Several interesting changes can be seen in examining the central grid profile with respect to time (see fig. 15). There is a definite change in the relative amount of rain-water in the lower regions of the cloud for the α = 4080 case.
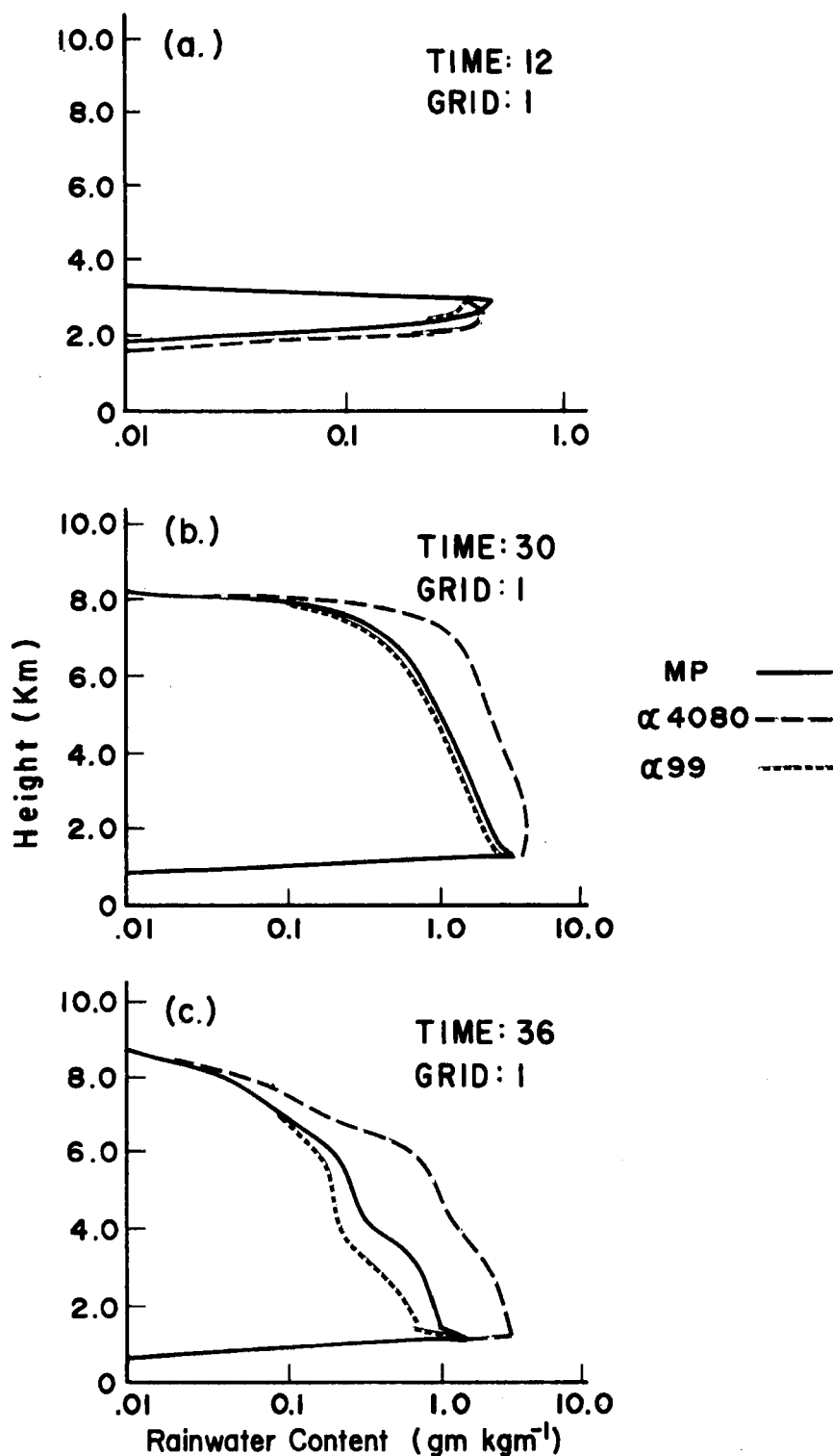
Fig. 15. A comparison of rainwater development in the central cloud column (grid 1). Rainwater content for 12, 30, and 36 minutes of cloud growth is shown for both the MP and ISWS α_{99} and α_{4080} cases.

At 12 minutes of cloud growth the large α case has shifted rainwater one grid level below the MP case. The small α case is significantly below the MP case at this time; however as time increases the differences between the MP case and that of large and small α values of the ISWS cases become more pronounced. After 30 minutes of the cloud growth, the α = 4080 ISWS spectra has produced substantially more rainwater throughout the depth of the cloud. As seen in Figure 15, we have at 6.0 km, 1.0 gm kgm^{-1} of rainwater for the MP case, whereas about 2.2 gm kgm^{-1} have been produced in the α = 4080 ISWS case. After 36 minutes of cloud growth (fig. 15c), there is nearly 3 to 4 times as much rainwater for the large α case as the MP case in contrast to 20-40% less rainwater in the small α case. At cloud base the rainwater is 40% greater than MP for the large α (1.8 gm kgm^{-1} vs 3.4 gm kgm^{-1}, respectively). This change represents a substantial increase in rainwater of the large α case over the MP case.

Examination of the horizontal structure of the cloud and profiles not directly in line with the central cloud axis, shows much more complicated patterns of precipitation and cloud water. These patterns result from more complex fields of motion away from the central core region. Early in cloud development the circulation within the cloud does not significantly affect the precipitation profiles. However, beyond 28 minutes of cloud growth marked effects upon
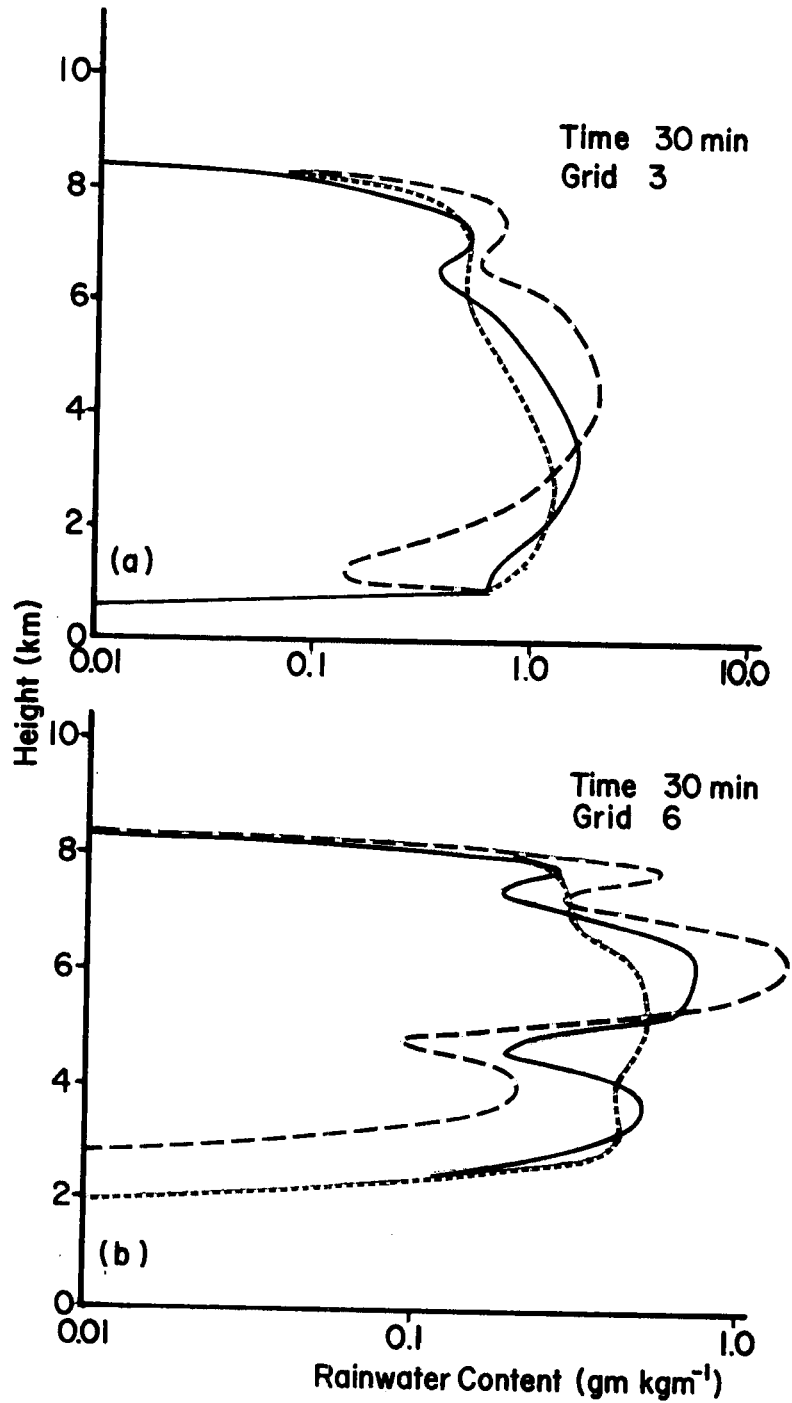
Fig. 16. A comparison of rainwater content at distances away from the central cloud core (grid 1) at 30 minutes of cloud growth. Rainwater profiles at 600 and 1200 meters from cloud center are shown.

the precipitation curves develop away from the central core. These effects are manifested by the large departures in the rainwater profiles from those of the central core. In regions of large variations of motion, the size spectra of particles become particularly important due to the strong influences of size on terminal velocity and hence upon rainwater content profiles. Smaller particles are more easily influenced by the air currents within a cloud; therefore, the physical effects of particle spectra are more pronounced in the region outside the central core as seen in Figure 16.

Vertical Velocity Profile

An example of the vertical velocity field after 33 minutes of cloud growth shows an updraft from 2 to 4 km above the surface at the center of the cloud (see fig. 17). The maximum updraft speed is 4 m sec^{-1} whereas the maximum downdraft is 11 m sec^{-1} at the 5.8 km level. A small change of vertical motion from the MP case is caused by the ISWS drop spectra using an α value of 99. The shift of speed is generally toward reduced upward motion and increased downward motion indicating that the new raindrop spectra does have an effect upon the vertical motion.

The raindrop spectra changes appear to have a smaller effect as the distance from the cloud core increases as shown in Figures 17b and 18b. Here at 600 meters from the
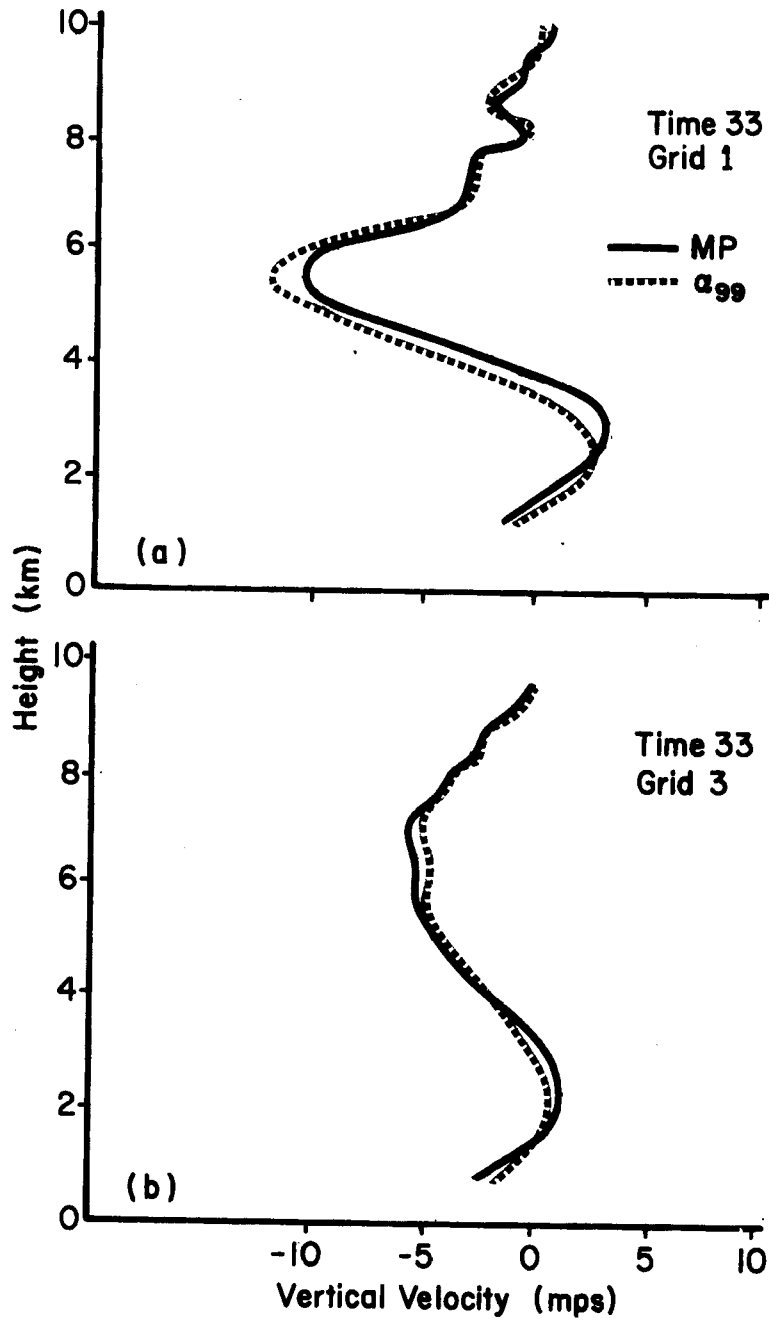
Fig. 17. Vertical velocity profiles for MP and ISWS cases
at 33 minutes of cloud growth at cloud center
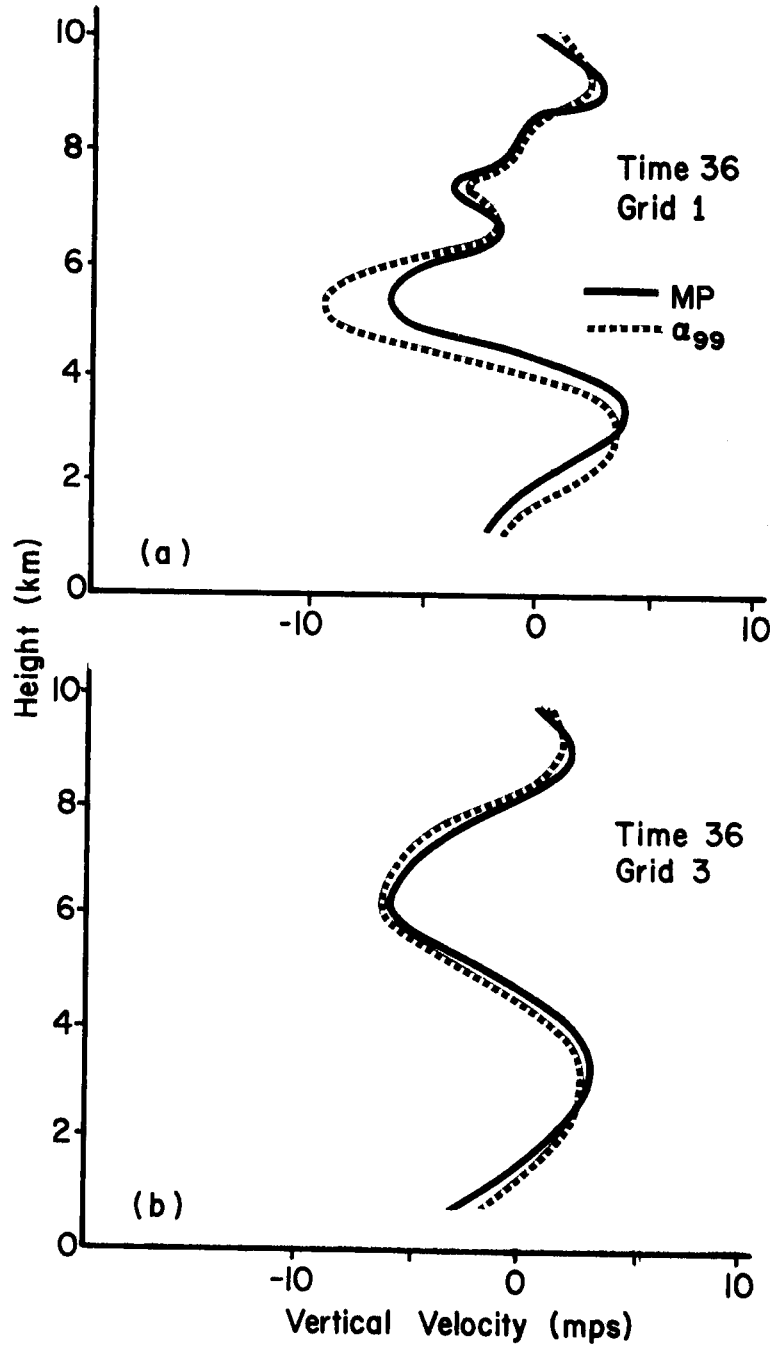(grid 1) and 600 meters from cloud center (grid 3).

Fig. 18. Vertical velocity profiles for MP and ISWS cases at 36 minutes of cloud growth at cloud center (a) and 600 meters from cloud center (b).

central core a very slight shift of velocity is evident.

The small shift toward cloud fringes may be due to smaller

liquid water contents in this region which would affect the

buoyant updraft to a lesser extent. The pattern of reduced

updraft at low levels is however still persistent. This

pattern may be characteristic of the decaying stage of

cloud development.

As cloud growth time increases to 36 minutes the verti-

cal motion profile shows a similar pattern of increased

central downdraft and somewhat decreased updraft (fig. 18).

The pattern of motion at grid 3 (fig. 18b) shows a more pro-

nounced change from updraft to downdraft as height increases;

however, the magnitude of change induced by the ISWS spectra

is smaller than in the cloud core.

In summary the shift toward increased downward motion

of the air in the cloud in the ISWS case may be a result of

increased water drag on upward vertical motion due to the

new drop size distribution. Thus the vigor of a developing

cloud may be directly affected by the drop spectra.

Model Sensitivity

Model sensitivity can be illustrated by the effects of

eddy diffusion of 80 m sec^{-1} in the rainfield which was

added to the Orville symmetric cloud model in November 1970

(Orville, 1971). This change produced significant shifts

of both the cloud and rainwater profiles of the same order

of magnitude as that produced by the Illinois State Water

Survey distributions. The net result of the cloud water

shift due to eddy diffusion is illustrated by Figure 19a.

Here we see that the original cloud water was about 1/2 that

of the new cloud at each level after 29 minutes of cloud

growth. We can also see that early stages of development at

5 and 17 minutes showed much less difference from the

original profile.

Rainwater sensitivity was also illustrated by the eddy

diffusion change. Rainwater was shifted to smaller values

in the new profile (fig. 19b). The changes became more

marked as cloud growth progressed from a few percent less

at 5 minutes to several times less than the original values

at 29 minutes.

With this example of model sensitivity, one can objec-

tively examine the changes in cloud and rainwater resulting

from the new raindrop distribution. Further more detailed

examination of model sensitivity to different sounding

cases representing changes in stability and consequent up-

draft strength should be made to determine the extent to

which other factors may affect the precipitation mechanism

of the model. Other stability conditions will also show

the degree to which precipitation may affect vigorous and

less vigorous clouds.
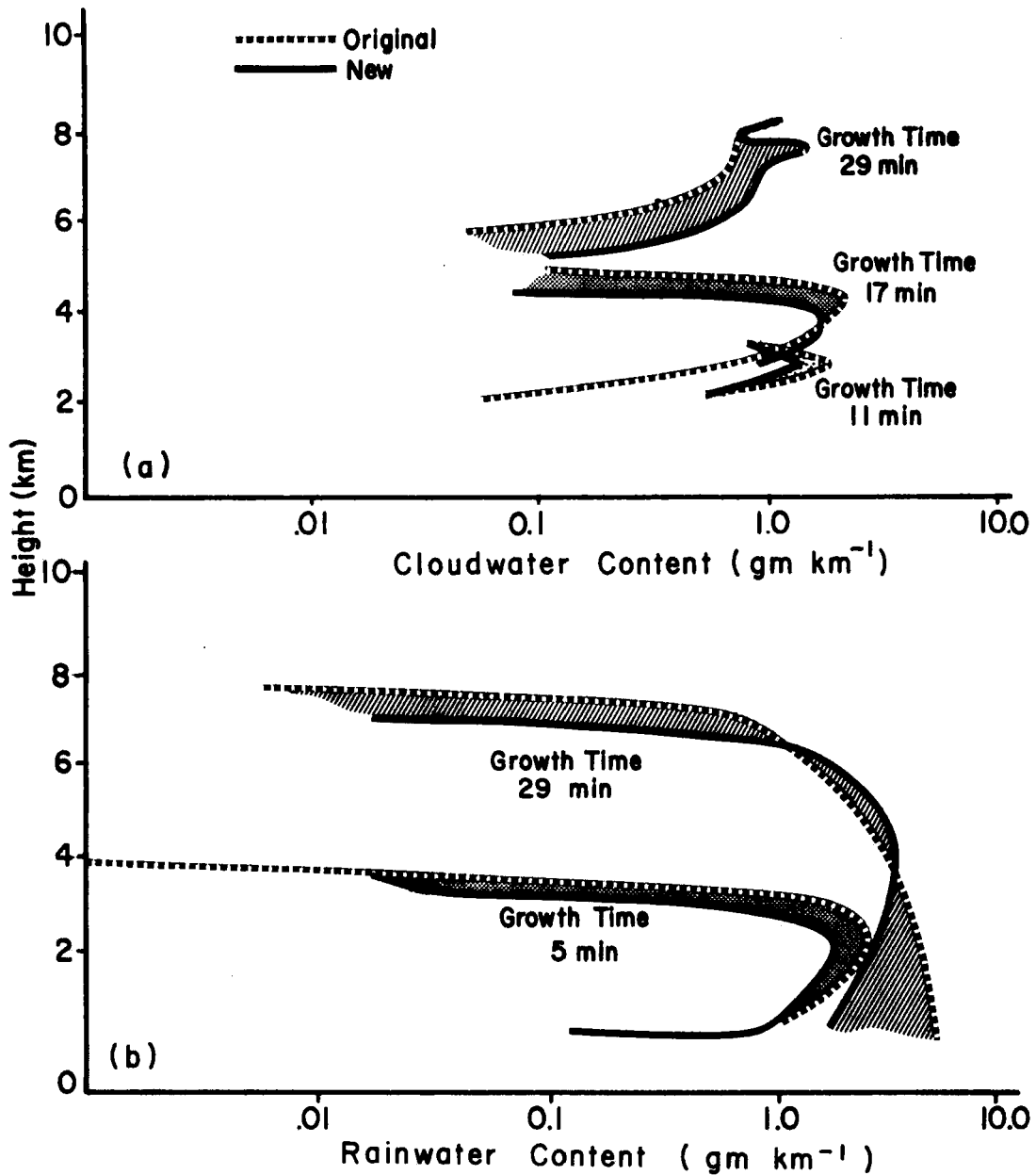
Fig. 19. An example of the sensitivity of the Orville
symmetric cloud model to Fickian diffusion of rain-
water. Three cloud growth times are compared
(11, 17, 29 minutes) to show changes in cloud
water (a) between cases with diffusion (new) and
without diffusion (original). Two growth times
(5 and 29 minutes) are compared to show changes
in rainwater profiles (b) with Fickian iffusion.

Summary of Results

Definite changes in rain and cloud water occurred in the Orville symmetric cloud model when different raindrop spectra were used in the hydrometeor growth equations. The shape and magnitude of these changes was similar to that introduced by the addition of eddy diffusion of rainwater. This suggests that the changes are well above model "noise level." Systematic shifts of cloud and rainwater profiles developed using the ISWS drop spectra. These shifts also were reflected by the systematic changes in the vertical motion profiles.

Surface rainfall in the ISWS drop spectra cases was significantly less than that of the MP case. These differences in rainfall from the MP case showed a nearly linear decrease at cloud center as the cloud developed. This decrease in percent change dropped linearly from 90% less than the MP rainfall (after 20 minutes of cloud growth) to 13% more than the MP rainfall (after 30 minutes of cloud growth).

VII. CONCLUSIONS

Drop Size Distribution

One basic conclusion which can be drawn from the literature is that there is no single log normal distribution that describes a drop size spectra of precipitation. Some observed drop spectra agree with the widely used Marshall-Palmer (1948) distribution; however, many others differ substantially from this distribution. Geographical location, precipitation generating mechanism (orographic, convective, warm, cold) and sounding characteristics appear to have direct influences on the shape of raindrop distributions. Natural processes within cloud such as condensation, coalescence, aggregation, and evaporation can significantly affect raindrop distributions which are observed below cloud base.

In most cases of observed raindrop spectra, significant deviations occur at the small end of the drop diameters. These deviations are generally orders of magnitude less than those numbers of drops predicted by the MP drop spectra. Observations of drop spectra in tropical orographic and non-orographic precipitation (Blanchard, 1953) and observations in temperate orographic and non-orographic precipitation (Ohtake, 1969) differ from the MP distribution. The number of small drops less than 1.0 mm and above 2.0 mm is generally less than that predicted by the empirical MP distribution.

Observations in clouds of raindrops have shown significant departures from the MP distributions at various levels within the cloud (Mee, 1968). In this case observations of tropical cumuli showed close agreement to the MP distribution at drop diameters above 2.0 mm; however, significant departures occurred below this size. Cloud top data agreed well with that of MP. From these in-cloud measurements one can conclude that there is a large variation of drop spectra throughout one of the simplest type of clouds. Thus very complicated processes may be involved in determining a given raindrop spectra.

Cloud Model Experiment

Significant changes in cloud water and rainwater profiles have resulted from the use of different raindrop spectra in a two-dimensional time dependent cloud model.

The differences from those values of rain and cloud water using a MP drop spectra increase as cloud growth time increases, thus indicating that the effect of different drop spectra may become more important as clouds develop. These differences are initially on the order of 5 to 10 percent of the original MP case and increase to 150 to 200 percent or more during the development of a cloud in the ISWS case.

Large variations in surface rainfall resulted from the use of different drop spectra in the model. These changes indicate that the particular type of drop spectra assumed

in the model does produce significant and systematical differences in surface precipitation.

The changes in cloud model results induced by different empirical drop spectra suggest that cloud models are significantly sensitive to the type of drop spectra used and must be "fine tuned" to improve their realistic representation of natural clouds.

VIII. RECOMMENDATIONS

Although many extensive observations of drop spectra exist, further more detailed studies should be made to determine those factors which will enable cloud models to rapidly describe specific rain, cloud, and ice particle distributions throughout the cloud. Future studies should follow two paths, laboratory (computer modeling) experimentation and field observations of precipitation and the cloud system from which it is formed. Bcth of these tasks will involve a tremendous effort, because of the need for background observations of cloud condensation nuclei, ice freezing nuclei, liquid water content, ice water content, temperature, dew point, stability and other pertinent cloud physics phenomena together with measurements of ice particle distributions and water particle distributions throughout a cloud and its environment. Not only will we need measurements of individual clouds but detailed measurements must be repeated in all major climatic, synoptic, and mesoscale conditions to compile a global picture of cloud development characteristics.

Together with field experimentation, computer modeling of the microphysical processes of condensation, coalescence, coagulation, aggregation, deposition and evaporation should be developed and verified by field observations. Examination

of a large number of cases under various conditions of condensation nuclei, freezing nuclei, seeding materials for both warm and cold clouds, soundings, and climatological and synoptic conditions, and mesoscale conditions will produce useful theoretical results which could be utilized by future cloud models.

The ultimate goal of the above program would be to produce detailed cloud drop and raindrop spectra which can be parameterized for fast single dimensional models and yet still represent real climatological, synoptic, mesoscale and microphysical properties pertinent to representative cloud modeling for a given time and place. Today the need for fast computation of cloud physics phenomena is obvious, due to the large amount of time and space required by detailed microphysical models which make them incompatible with larger synoptic scale numerical prediction models.

Dependence upon one observed drop spectra may be an unfortunate over-simplification of current cloud models. Greater effort is needed to fine-tune cloud microphysical parameterizations to observed natural clouds. A thorough documentation and analysis of cloud properties such as temperature, dewpoint, liquid water content, cloud water content, ice water content, particle spectra (rain, cloud, ice) and vertical motion throughout the cloud and its

surrounding environment are needed today to adjust or "tune" current cloud models. Model sensitivity to various parameters currently assumed should be examined under various sounding conditions. This would enable determination of those factors which may seriously affect the cloud model under various stability conditions.

Through the direct interaction of field observations and model adjustment, we can improve our understanding of cloud physics and produce more realistic cloud models. Better cloud models in turn will help us further understand cloud and precipitation mechanisms and their interaction with their environment. Thus, we can better understand individual and net effects of clouds and precipitation on the larger scale mechanisms of momentum and heat exchange in the atmosphere. Through better understanding of these small scale "trigger" interactions with the larger scale phenomena, we will be able to improve our prediction of the weather and ultimately control it.

REFERENCES

Adderly, E., 1953: Growth of Raindrops in Clouds. Quarterly Journal of the Royal Meteorological Society. Vol. 79, p. 380-389.

Battan, L. J., 1953: Observations on the Formation and Spread of Precipitation in Convective Clouds. Journal of Meteorology. Vol. 10, p. 311-324.

Battan, L. J., 1960: Radar Meteorology. University of Chicago Press.

Berry, E. X., 1968: Modification of the Warm Rain Process. Proc. First National Conference on Weather Modification, Albany, N. Y., American Meteorological Society, p. 81-88.

Blanchard, D. C., 1948: Observations on the Behavior of Water Drops at Terminal Velocity in Air. GE Laboratory Occasional Report No. 7, Contract 36-039-32427.

Blanchard, D. C., 1953: Raindrop Size Distributions in Hawaiian Rains. Journal of Meteorology. Vol. 1, p. 452-461.

Carlson, P. E., 1968: Measurement of Snow by Radar. Proceedings of the 13th Radar Conference, Boston, A.M.S., p. 384-387.

Davis, L., and A. Weinstein, 1968: A Parameterized Model of Cumulus Convection. Department of Meteorology, Penn. State University.

Duncan, A. D., 1966: The Measurement of Shower Rainfall Using an Airborne Impactor. Journal of Applied Meteorology. Vol. 2, p. 198-204.

Fujiwara, M., 1968: A Study of Raindrop Size Distributions. Ph.D. Thesis. Meteorological Research Institute, Suginami, Tokyo, Japan.

Gentry, R. C., 1971: Progress on Hurricane Modification Research, October 1969 to October 1970. To be published in the Proceedings of the 12th Interagency Conference on Weather Modification, 28-30 October 1970.

Gunn, K. L., 1952: The Effect of Accretion on Clouds Through Which Rain Is Falling. Geophys. Res. Paper, No. 13, p. 65-69.

REFERENCES (Continued)

Gunn, K. L., and J. L. Marshall, 1958: The Distribution With Size of Aggregate Snowflakes. Journal of Meteorology. Vol. 15.

Hardy, K. R., 1963: The Development of Raindrop Size Distributions and Implications Related to Physics of Precipitation. Journal of Atmospheric Science. Vol. 20, p. 299-312.

Imai, I. M., and M. Fujiwara, 1955: Radar Reflectivity of Falling Snow. Papers in Meteorology and Geophysics. Japan, Vol. 6, p. 130-139.

Jones, D. M. S., 1959: The Shape of Raindrops. Journal of Meteorology. p. 504-510.

Jones, D. M. S., and E. Mueller, 1960: Z-R Relations from Drop Size Data. Proceedings 8th Wea. Radar Conference, AMS, Boston. p. 498-504.

Jones, et al., 1968: Raindrop Spectra for Seeded and Unseeded Showers in Arizona. Proceedings 1st National Conference on Weather Modification. Albany, N. Y., p. 99-106.

Kessler, E., 1969: On the Distribution and Continuity of Water Substance in Atmospheric Circulations. Meteorological Monograms. Vol. 10, No. 32.

Kinzer, G. D., and R. Gunn, 1951: The Evaporation, Temperature, and Thermal Relaxation Time at Freely Falling Water Drops. Journal of Meteorology. Vol. 8, p. 71-83.

List, R. J., 1951: Smithsonian Meteorological Tables. Smithsonian Institution, Washington, D.C.

Langmuir, I., 1948: The Production of Rain by Chain Reaction in Cumulus Clouds at Temperatures Above Freezing. Journal of Meteorology. Vol. 5, p. 175-460.

Langleben, 1954: Terminal Velocity of Snow Aggregate. Quarterly Journal of the Royal Meteorological Society. Vol. 80, p. 174-181.

Laws, and Parsons, 1954: The Relation of Raindrop Size to Intensity. Transcript of American Geophysical Univ. 24 Part II. p. 452-460.

REFERENCES (Continued)

Lhermitte, R. M., 1966: Application of Pulse Doppler Radar
    Techniques to Meteorology. Bulletin of the A.M.S.
    Vol. 47, No. 9.

Litvinow, I. W., 1958: Size Distribution of Raindrops From
    Melting Hail. Bulletin Isvestiya Acad. Sci. USSR.
    Geophys. Ser. p. 513-518.

Marshall, J. S., and W. Mck. Palmer, 1948: The Distribution
    of Rainfall with Size. Journal of Atmospheric Science.
    Vol. 5.

Mee, T. R., and D. M. Takeuchi, 1968: Numerical Glaciation
    and Particle Size Distribution in Marine Tropical
    Cumulus. M.R.I. Report for. E.M.B., ESSA. MR 168,
    FR 823.

Mueller, E. A., 1962a: Investigation of the Quantitative
    Determination of Point and Areal Precipitation by Radar
    Echo Measurements. Second Quarterly Technical Report.

Mueller, E. A., 1962b: Investigation of the Quantitative
    Determination of Point and Areal Precipitation by
    Radar Echo Measurements. Second Quarterly Technical
    Report.

Mueller, E. A., 1966: Radar Cross Sections From Drop Size
    Spectra. Ph.D. Thesis. University of Illinois,
    Urbana, Illinois. Fourth Quarterly Technical Report.

Murray, F. W., 1970: Numerical Models of a Tropical Cumulus
    Cloud With Bilateral and Axial Symmetry. Monthly
    Weather Review. p. 14-28.

Murray, F. W., 1971: Personal Correspondence.

Nakaya, J., 1951: The Formation of Ice Crystals. Compendium
    of Meteorology, Boston, American Meteorology Society.
    p. 207-220.

Ohtake, T., 1969: Observations of Size Distributions of
    Hydrometeors Through Melting Layer. Journal of
    Atmospheric Science. Vol. 26, No. 3, May 1969.

Ohtake, T., 1970: Factors Affecting the Size Distribution
    of Raindrops and Snowflakes. Journal of Atmospheric
    Science. August 1970.

REFERENCES (Continued)

Orville, H. D., 1965: A Numerical Study of Cumulus Clouds Over Mountainous Terrain. Journal of Atmospheric Science. p. 684-699.

Orville, H. D., 1971: Personal Correspondence. January 1971.

Orville, H. D., and J. Y. Liu, 1969: Numerical Modeling of Precipitation and Cloud Shadow Effects on Mountain-Induced Cumuli. Journal of Atmospheric Science. p. 1283-1298.

Rigby, E. C., J. S. Marshall and W. Hitschfeld, 1954: The Development of the Size Distribution of Raindrops During Their Fall. Journal of Meteorology. p. 363-372.

Sheets, R. C., 1969: Computations of the Seedability of Clouds in a Hurricane Environment. Project STORMFURY Annual Report 1968.

Simpson, J., and V. Wiggert, 1969: Models of Precipitating Cumulus Towers. Monthly Weather Review. Vol. 97, No. 7.

Spilhaus, A., 1948: Drop Size, Intensity and Radar Echoes of Rain. Journal of Meteorology. Vol. 5, p. 161-164.

Sekhon, R. S., and R. Stravastavv, 1970: Snow Size Spectra and Radar Reflectivity. Journal of Atmospheric Science. Vol. 27, p. 299.

Stravastavv, R. S., 1967: A Study of the Effects of Precipitation on Cumulus Dynamics. Journal of Atmospheric Science. Vol. 24.

Warner, J., 1969: The Microstructure of Cumulus Cloud. Part I. General Features of the Droplet Spectrum. Journal of Atmospheric Science. p. 1049-1059.

Warner, J., 1970: On Steady State One Dimensional Models of Cumulus Convection. Journal of Atmospheric Science. p. 1035-1040.

Weinstein, A., and McCready, 1969: An Isolated Cumulus Cloud Modeling Project. Journal of Applied Meteorology. Vol. 8, p. 936-949.

Weinstein, A., 1970: A Numerical Model of Cumulus Dynamics and Microphysics. Journal of Atmospheric Science. Vol. 27, No. 2.

REFERENCES (Continued)

Wisner, C., 1970: A Numerical Model of a Cumulus Cloud.
    M.S. Thesis, Institute of Atmospheric Sciences, South
    Dakota School of Mines and Technology.